MODEL AND ANALYSIS OF BURST PACKET LOSSES AND PACKET DELAYS IN IP NETWORKS USING MARKOV CHAINS

A Dissertation by

Murali Krishna Kadiyala

Master of Science, Wichita State University, 2005

Submitted to the Department of Electrical Engineering and Computer Science
and the faculty of the Graduate School of
Wichita State University
in partial fulfillment of
the requirements for the degree of
Doctor of Philosophy

May 2011

MODEL AND ANALYSIS OF BURST PACKET LOSSES AND PACKET DELAYS IN IP NETWORKS USING MARKOV CHAINS

The following faculty members have examined the final copy of this dissertation for form and content, and recommend that it be accepted in partial fulfillment of the requirement for the degree of Doctor of Philosophy with a major in Electrical Engineering.

Ravi Pendse, Committee Chair

Neeraj Jaggi, Committee Co-Chair

Edwin Sawan, Committee Member

John Watkins, Committee Member

Krishna Krishnan, Committee Member

Daowei Ma, Committee Member

Accepted for the College of Engineering

Zulma Toro-Ramos, Dean

Accepted for the Graduate School

J. David McDonald, Dean

DEDICATION

To Amma-Nanna, Lord SriKrishna and Jagadguru Sri AadiShankaracharya,
and my favorite Goddess SriLalitha

Avidyanaam Antastimira Mihira Dweepanagareem
Jadaanaam Chaitanya Stabakamakaranda Shrutijhareem
Daridraanaam Chintaamani Gunanikaa; Janmajaladhau
Nimagnaanaam Damstraa Muraripu Varaahasya Bhavathi

- Soundarya Lahari

ACKNOWLEDGEMENTS

I have no words to express my gratitude for Lord SriVenkateshwara for his mercy and blessings showered on me in every walk of my life.

I am indebted to my advisor Dr. Ravi Pendse for his constant support and encouragement during my journey towards fulfilling my ambition of acquiring a doctorate in engineering. He taught me everything of computer networking right from basics to an advanced level of achieving my PhD. But for him, I would not have pursued my doctoral study at WSU after my Masters. He provided me all freedom and opportunities to participate in several conferences and develop as a researcher and lead.

I am grateful to my co-advisor Dr. Neeraj Jaggi for his valuable time and guidance in my research work. I am immensely benefitted by his knowledge and experience in improving my abilities in drafting my research papers. I thank him for giving me the opportunity to participate in the Innovation Engineering Leadership Workshop.

I thank Dr. Edwin Sawan, Dr. John Watkins, Dr. Krishna Krishnan, and Dr. Daowei Ma for their participation in the committee and for their valuable suggestions and time.

I am grateful to my uncle Dr. Kamesh Namuduri and my sister Dr. Savitha Namuduri who are instrumental in my coming to the United States of America for higher education. Their blessings have enabled me complete my PhD. I extend my special love to my niece Shalini.

I express my sincere thanks to Dr. Zulma Toro-Ramos, Dean of College of Engineering, and Ms. Debra Franklin, Director of Center for Innovation and Enterprise Engagement for their motivation and support for my participation in the management development program 'Innovation Engineering Leadership' arranged by WSU for the first time. I was the only PhD student among the workshop participants.

ACKNOWLEDGEMENTS (continued)

I thank all members of the University Administration who have been very friendly and cooperative during my studies at WSU.

I thank my senior colleagues Mr. Amarnath Jasti, Mr. Vijay Ragothaman, and Mr. Nagaraja Thanthry for their help and also for the great time we had together at WSU. I also thank Dr. Patricia Best and my colleagues at the Cisco Technical Research Center, WSU.

I thank Jayesh and Samir for their contribution in preparing this dissertation report.

I thank all my friends who directly or indirectly helped me in successfully completing this endeavor, and for their immense love.

I also take this opportunity to express my thanks to the Officials of the University Police Department, WSU, for providing a safe and secure University Campus. My thanks also go to the armed forces of USA and India safeguarding both the nations round the clock.

It gives me pleasure to express my thanks to my loving sister Radhika and brother-in-law Prasad for their affection and encouragement, and my love for my niece Adithi and nephew Chaitanya. I also express my special thanks to Dipti. My thanks also go to the victorious Indian Cricket Team who won Cricket World Cup on Apr 2, 2011 just a few days before my defense.

I am grateful to the stalwarts of earlier ages – Aacharya Chanakya, Emperor SriKrishnaDeva Raya, Chatrapati Shivaji, Andhra Kesari Sri Tanguturi Prakasam Pantulu, and Dr. N. T. Rama Rao (ex-Chief Minister of Andhra Pradesh, India) who have been a great source of inspiration, energy, and encouragement for me in tiding over all difficulties in life.

I am deeply indebted to my beloved parents for their abundant love, affection, and blessings, and for giving me a wonderful childhood and carving me out as a good human. I owe all my successes to my parents.

ABSTRACT

The classic problem of communication networks such as increase in packet delays and packet losses regains significance with the evolution of a new variety of communication networks and networking protocols. Packet delays in wired networks like the Internet were very well analyzed in the past. However, the packet delays in ad hoc networks were not thoroughly studied, especially, with respect to issues like the effect of medium access control (MAC) layer delays on the upper layer delays associated with the packet transmission process, the packet service-time, and packet end-to-end delay. Similarly, the packet losses in wired networks were analyzed using empirical models based on Markov chains. These models lack the ability to describe the response of an Internet router for different packet arrival patterns. For the networks experiencing frequent burst losses, it is very important to analyze the effect of packet inter-arrival time on such losses. This calls for a set of well-defined analytical models which can help in identifying the parameters responsible for the increase in packet delays and packet drops. Such models also extend to devise new network protocols and mechanisms, and improve the network throughput. This dissertation addresses the requirement of such models. The first part proposes an analytical model to describe packet delays in ad hoc networks and highlights the effect of MAC delays on route discovery time and node's packet service-time. The second part presents a semi-Markov process based model to analyze the wireless LANs (WLANs) and the MAC protocols such as the IEEE 802.11 Distributed Coordination Function (DCF) used in the IEEE WLANs. The third part presents an empirical model to describe the burst losses in Voice over Internet Protocol (VoIP) caused by queue overflows at the Internet routers. As an extension to this dissertation, an analytical model describing the combined effect of packet arrival-rate, packet service-rate, and the queue capacity on burst losses is also presented as future work.

TABLE OF CONTENTS

Chapter Page

TABLE OF CONTENTS (continued)

LIST OF TABLES

Table Page

LIST OF TABLES (continued)

Table Page

LIST OF FIGURES

LIST OF ABBREVATIONS/NOMENCLATURE

ACK	Acknowledgement
BEB	Binary Exponential Mechanism
BO	Backoff- interval
CBR	Constant Bit Rate
CTMC	Continuous-Time Markov Chain
CTS	Clear To Send
CWmax	Maximum Contention Window
CWmin	Minimum Contention Window
DCF	Distributed Coordination Function
DIFS	Distributed Inter-Frame Space
DSSS	Direct Sequence Spread Spectrum
DTMC	Discrete-Time Markov Chain
EDCA	Enhanced Distributed Channel Access
FHSS	Frequency Hopping Spread Spectrum
IP	Internet Protocol
LAN	Local Area Network
MAC	Medium Access Control
MC	Markov Chain
RREP	Route REPly
RREQ	Route REQuest
RERR	Route ERRor
RTS	Request To Send

LIST OF ABBREVATIONS/NOMENCLATURE (continued)

SIFS	Short Inter-Frame Space
UDP	User Datagram Protocol
VoIP	Voice over Internet Protocol

Chapter 1

Introduction and Preview

1.1 Introduction

The packet transmission process forms the basis for communication networks [1, 5, 6]. The packet transmission delay gains importance in the networks implementing real-time transmissions. With an increase in the packet transmission delay, the time required to accomplish the task also increases, and the task fails when the packet transmission delay exceeds the threshold value. For instance, if the packet service-time and packet end-to-end delays in the real-time application such as Voice over Internet Protocol (VoIP) exceed the threshold, then the VoIP application fails because of the unclear and disrupted voice heard by the end users [2, 3]. Similarly, certain network tasks require communication and coordination among multiple network nodes in which packet service-time and packet end-to-end delay must be very low for the successful implementation of the task. Hence, the analysis of the packet transmission process along with the associated delays helps in identifying the major delay components in the process. Furthermore, the new varieties of communication networks and the network protocols are always associated with different types of delays [7–9]. Hence, a well-defined model is required to analyze the performance of the communication protocols in the networks. Such models not only help in selecting the best available protocol for the network, but also help in designing new protocols that can improve the network throughput.

The burst packet losses in communication networks cause the loss of information [2, 3]. In a real-time application such as VoIP, these losses degrade the quality of voice by disrupting the speech patterns available from the received packets. This is due to the inability of the voice decoder at the receiver end to interpolate the lost (consecutive) packets from the received packets. Hence, the burst losses must be regulated in the communication network. In order to do so, a detailed analysis of burst losses must be performed through a well-developed analytical model [2, 3]. Such a model not only helps in reasoning the causes of burst losses, but also helps in assessing the network resources required for regulating burst losses to smaller (acceptable) lengths. This dissertation addresses the above mentioned issues.

1.2 Dissertation Overview and Contribution

This dissertation is broadly divided into three parts each addressing an essential problem in computer networks using a mathematical model.

The first part of this research proposes an analytical model to describe packet delays in stationary and mobile ad hoc networks, and highlights the effect of MAC delays on route discovery time and node packet service-time [5, 6].

Because the network delays and throughput are largely dependent on the MAC protocols such as the IEEE 802.11 Distributed Coordination Function (DCF) protocol and the IEEE 802.11e Enhanced Distributed Channel Access (EDCA) protocol, the selection of an appropriate MAC protocol is a critical requirement [1]. An efficient mathematical model is, hence, required in order to better analyze the performance of MAC protocols. The second part of this dissertation presents a semi-Markov process based model to analyze the MAC protocols and the IEEE wireless local area networks (WLANs) employing these protocols. The usage of this model is illustrated with the performance analysis of DCF protocol [1].

The third part of the dissertation presents an empirical model for describing burst losses in Voice over IP (VoIP) on the Internet routers. It illustrates the effect of packet inter-arrival times on burst losses [2, 3]. This model is useful in analyzing the burst loss patterns for a variety of traffic in a specific network or at a network device [2, 3].

An analytical model has also been presented which discusses the combined effect of packet arrival-rate, packet service-rate, and queue capacity on the length of burst losses. This model helps in evaluating the router resources required to restrict the burst losses to specific lengths [4].

The models proposed in this dissertation highlight the essential factors associated with the three network problems. These models also help in identifying the future requirements in developing new protocols and mechanisms for reducing the packet delays in ad hoc networks and for reducing burst losses for real-time applications.

1.3 Dissertation Outline

The remaining part of this dissertation consists of six chapters. Chapter 2 presents the literature survey on the IEEE 802.11 DCF MAC protocol. Chapter 3 presents an analytical model for packet service-time in saturated ad hoc networks and describes the impact of MAC frame delays on the packet service-time. Chapter 4 presents the semi-Markov process based model for the performance analysis of the IEEE 802.11

DCF WLANs. Chapter 5 presents the literature survey on burst losses in Voice over Internet Protocol (VoIP). Chapter 6 models the burst losses in VoIP as a semi-Markov process. Chapter 7 presents the conclusions of this dissertation and the scope for future work. In this direction, an analytical model for the burst losses in real-time applications using Continuous-Time Markov Chains (CTMC) is also presented as an extension to the dissertation. The validation of the model has to be carried out.

Chapter 2

Literature Survey on the IEEE 802.11 DCF Protocol

2.1 Introduction

This chapter presents the literature survey on the IEEE 802.11 Distribution Coordination Function (DCF) protocol in three sections followed by an outline of the research work presented in chapters three and four.

2.2 Performance Analysis of the IEEE 802.11 DCF MAC Protocol

Bianchi [10] analyzed the saturation throughput of the IEEE 802.11 DCF protocol using a two-dimensional Markov chain. The backoff stages and the backoff counters represent two dimensions of the Markov chain. The author's analysis was primarily based on two parameters: the transmission probability and the collision probability. The effect of these parameters on the protocol's saturation throughput was analyzed. Shabdiz and Subramaniam [11] analyzed the saturation throughput of the IEEE 802.11 DCF MAC for finite loads based on the two-dimensional Markov chain proposed in [10]. Kwak et al. [12] analyzed the stability and performance of the IEEE

802.11 DCF protocol's Binary Exponential Backoff (BEB) mechanism under saturation conditions. The authors assumed a fixed number of nodes and a fixed network load for this analysis. The backoff stages of an ad hoc node were modeled using a one-dimensional Markov chain. However, the state holding time and its effects were not included in the analysis. Chen and Li [13] analyzed the performance of a new packet transmission mechanism, which is the hybrid of basic access and the request-to-send/clear-to-send (RTS/CTS) mechanism. The authors evaluated the saturation throughput of this mechanism for variable packet lengths. The packet length was assumed to follow a general probability function. Foh and Tantra [14] further extended the model in [10]. The authors assumed that the channel access probability and station collision probability depend on the status of communication channel, and proposed their analytical model. Dong and Pravin Varaiya [15] introduced the concept of the virtual slot for analyzing the IEEE 802.11 local area networks (LANs). They defined the virtual slot as the time interval between two consecutive backoff counter decrements of non-transmitting stations. The authors' analysis specifically focused on lossy channels under saturation conditions.

2.3 MAC Queuing Models

Tickoo and Sikdar [16] analyzed MAC layer queueing delays in the IEEE 802.11 wireless LANs. The network nodes are modeled as discrete time G/G/1 queues. A closed-form expression for delay and queue-length characteristics was obtained for each node. The distribution of the packet service-time was derived through the channel access delay, the packet collision period, and the backoff period. This research work was extended to study the effect of a finite load on collision rates and queue utilization in [17]. Sitharaman [18] modeled the MAC queues in the IEEE 802.11 ad hoc networks, and analyzed the frame's service-time patterns. He emphasized that the service time follows Poisson distribution in scenarios, including hidden nodes and neighborhood "menace". Also, the inter-arrival time at the next hop nodes was observed to follow exponential distribution. The author proposed a general state transition diagram for the IEEE 802.11 DCF MAC protocol, which along with the two-dimensional Markov chain [10], was used for his analysis. Abdrabou and Zhuang [19] studied the patterns of service time for the IEEE 802.11 saturated single-hop ad hoc networks. They demonstrated that (a) the number of successful transmissions per unit time interval follows Poisson distribution, and (b) the service-time patterns closely follow geometric distribution. Also, the authors propose discrete-time queuing for modeling the queues of the IEEE 802.11 ad hoc networks during saturation conditions. Kalil et al. [20] analyzed the packet end-to-end delay in the IEEE 802.11 multi-hop networks. The authors emphasized the requirement for effective queuing techniques for reducing packet loss probability and the packet end-to-end delay. They also developed a Markovian model for evaluating the queuing mechanism they proposed.

2.4 Enhanced IEEE 802.11 DCF

Li and Battiti [21] analyzed the IEEE 802.11 DCF protocol and proposed various modifications to support differentiated services. The authors associated parameters such as minimum contention window size and the packet payload size with traffic priorities. They further examined the throughput and packet delay in the transmissions. Zhu and Chlamtac [22] introduced differential service parameters into the two-dimensional Markov chain [10], and analyzed the IEEE 802.11 DCF protocol throughput under saturation conditions. Heusse et al. [23] demonstrated the performance anomaly of the IEEE 802.11*b* in WLANs, and analyzed the protocol using Markov chains [10]. The authors assumed saturated sources and a single modulation rate. They illustrated that the network performance degrades if a node operates at a lower bit rate, even though all other nodes operate at a very high bit rate. They described this characteristic as an inherent feature of the CSMA/CA mechanism to guarantee an equal and long-term channel access probability to all network nodes. Cantieni et al. [24] analyzed fairness issues of the IEEE 802.11*b* in multirate environments. The authors proposed a metric called the fairness index for the protocols that permit the network nodes to gain equal channel occupation times. The authors evaluate their mechanism in terms of throughput and MAC delays for various network configurations. Grilo and Nunes [25] examined the QoS standards of the IEEE 802.11*e*. They analyzed and compared the enhanced DCF and hybrid coordination function modes with legacy DCF and Point Coordination Function (PCF) protocols, respectively. The comparison was based on simulation results. Velloso et al. [26] studied the effect of mobility and traffic load variations on voice packet transmissions in the IEEE 802.11 DCF networks. This examination was conducted in terms of delay, jitter, consecutive losses, and loss rate.

In the research work discussed in sections 2.2 through 2.4, the effect of MAC delays on the node packet service-time in stationary and mobile ad hoc networks was not well-conceived and modeled. Similarly, the effect of these delays on other delays such as route discovery time and queuing delays were also not modeled. Furthermore, the performance analysis of the IEEE 802.11 DCF protocol was primarily carried out through a two-dimensional Markov chain proposed in [10] with the complexity of order $O(2^m)$. In this dissertation, the effect of MAC delays on packet service-time, route discovery time, and queuing delays are thoroughly analyzed and modeled in chapter three. Furthermore, in chapter four the BEB mechanism of the IEEE 802.11 DCF protocol is represented as a semi-Markov process by modeling its backoff stages and backoff interval as the states of the semi-Markov process and their state holding times, respectively. The proposed model has a reduced number of states to the order $O(m)$ compared to that of two-dimensional Markov chain [10] of order $O(2^m)$. Thus this dissertation provides a simpler approach for computing the parameters of interest such as conditional collision probability, the node's packet transmission probability, and saturation throughput. Additionally, the computation time for obtaining the stationary probabilities of the semi-Markov process is approximately one-tenth of that incurred by Bianchi's model. Thus, the semi-Markov process provides an accuracy close to Bianchi's model with lower complexity and less computation time, and, thus, is more suitable for analyzing complex protocols such as the IEEE 802.11e with EDCA [27]. This model finds a significant application in pervasive wireless LANs [28, 29], such as ad hoc networks or sensor networks, employed for mission-critical applications in which every node is required to assess the conditional collision probability and saturation throughput of the network before transmitting a packet. This model assumes that the network nodes are aware of network size [30, 31].

Chapter 3

Analytical Model for Packet Service-Time in Wireless Ad Hoc Networks

3.1 Introduction

Packet service-time is an important parameter in the analysis of real-time transmissions in wireless ad hoc networks. With an increase in the network size (number of nodes in the network), the MAC contention increases leading to more collisions and cross-transmissions finally resulting in higher packet service-time in the network [5, 6]. This chapter presents an analytical model for MAC frame service-time and node packet service-time in stationary and mobile ad hoc networks.

3.2 Analytical Model For Average Packet Service-Time in Ad Hoc Networks

This section presents an analytical model for packet service-time in saturated ad hoc networks. The packet service-time in ad hoc networks primarily depends on MAC and routing delays [5, 6]. If the source node has a route to the destination, then the node's average packet service-time equals the MAC frame service-time. If n_{tr} is the average number of transmission attempts required for successfully transmitting a frame at the MAC layer, then the MAC frame service-time D_S^M is given by [5, 6]

$$
\begin{aligned}
D_S^M &= [(n_{tr} - 1) * T_{uRTS}] + T_{sRTS} && (3.2.1)\\
&= (n_{tr} - 1)[DIFS + RTS + \mu] + (DIFS + RTS + CTS)\\
&+ \; DATA + ACK + 4\mu + 3SIFS + \sum_{j=0}^{(n_{tr}-1)} \{E[BO_j] + E[CR_j]\} && (3.2.2)
\end{aligned}
$$

$E[BO_j]$ represents the expected value of backoff interval for the j^{th} backoff-stage, and $E[CR_j]$ represents the expected value for the time spent in cross-transmissions for j^{th} backoff-stage. When the number of neighbors within a node's transmission range increases, the number of transmission attempts required for successful delivery of the frame, and the backoff-time and cross-transmission time also increase.

The average time spent by a node in successful transmission of a MAC frame T_{sRTS} is given by [5, 6]

$$T_{sRTS} = DIFS + E[BO_j] + E[CR_j] + RTS + CTS + DATA + ACK + 4\mu + 3SIFS$$

where $DIFS$ is the distributed inter-frame space, $E[BO_j]$ is the expected value of backoff-interval in the j^{th} backoff-stage in the frame transmission process, $E[CR_j]$ is the expected value for the time spent in cross-transmissions, RTS is the time required for RTS frame transmission, CTS is the time required for CTS frame transmission, $DATA$ is the time required for data transmission, $SIFS$ is the short inter-frame space, and μ is the propagation delay of the MAC frame.

The average time spent by a node in an unsuccessful transmission T_{uRTS} is given by [5,6]

$$T_{uRTS} \;=\; DIFS + E[BO_j] + E[CR_j] + RTS + \mu$$

The queuing-delay for i^{th} frame in the MAC queue $D^M_{Q(i)}$ is given by [5–7]

$$D^M_{Q(i)} = (i-1) \times D^M_S \tag{3.2.3}$$

Therefore, the average service-time $T^s_{S(i)}$ for the i^{th} frame in the queue in a stationary network is given by [5,6,8]

$$T^s_{S(i)} = i \times D^M_S \tag{3.2.4}$$

The packet service-time in mobile ad hoc networks is greater than that in the stationary networks. This difference is caused by the route discovery time associated with the route discovery processes initiated as a response to the frequent link failures. The source nodes initiate the route discovery process to reach the unknown destinations [5, 6]. The time spent in a single route discovery process is equal to $(D^R_{req} + D^R_{repTout})$, where $D^R_{req} = D^M_S$ and the size of $DATA$ equals the route request packet (RREQ). Suppose that nRQ is the average number of route discoveries initiated to reach the destination. Then, the route discovery time D^R_{RDt} is given by [5,6]

$$D^R_{RDt} = nRQ(D^R_{req} + D^R_{repTout}) \tag{3.2.5}$$

where $D^R_{repTout}$ is the average RREP time-out period at the network layer.

For the mobile ad hoc networks characterized with node mobility and frequent link drops, the average packet service-time $T^m_{S(i)}$ for the i^{th} packet is the sum of the route discovery time and the MAC frame servicing-delay [5]. If x out of i packets require new path to reach the destination, then

$$T^m_{S(i)} = x(D^R_{RDt} + D^M_S) + (i-x)D^M_S \tag{3.2.6}$$

Therefore, the packet service-time $T_{S(i)}$ in an ad hoc network is the minimum in stationary networks for the first packet in the node's queue, once the route to the destination is already established, and $E[CT_j]$ is equal to zero. The packet service-time in ad hoc networks is maximum in mobile networks for the last packet in the queue with n_{tr} equal to $(m+1)$, $E[CT_j]$ equal to zero, and x equal to l.

The lower and upper bounds of packet service-time effects the lower and upper bounds of frame queuing delays, frame inter-arrival times, and the route discovery time in ad hoc networks as discussed in [7–9].

3.3 Simulations and Results

Table 3.1: Various parameters and their values used for simulations [6].

Parameter	*Value*
Physical Layer Standard	DSSS
RTS	44bytes
CTS	38bytes
DATA	500bytes
ACK	38bytes
Slot-time	20μs
DIFS	50μs
SIFS	10μs
Data Rate	100kbps
Routing Protocol	AODV
Network Size	(10,20,30,40,50) nodes
Node Transmission Range	250m
Terrain Area	200m x 200m
Simulation Time	90s

The simulations were performed to study the effect of network size on MAC delays,

Table 3.2: MAC transmission statistics for a network size of 10 nodes [6]

SID	TTA	BS	CT	$TTBS(ms)$
1	4	0	1	2.350
		1	8	27.026
		2	39	131.070
		3	21	126.692
2	2	0	32	94.130
		1	3	15.288
3	1	0	1	11.608

and the effect of MAC frame service-time on node packet service-time in saturated stationary ad hoc networks [6]. These simulations were carried out on a network simulator-2 (ns2). By varying the number of nodes in the saturated IEEE 802.11 DCF network from 10 through 50 in steps of 10, the variation in medium access delays and their impact on the packet service-time were closely studied. The parameters used for the simulations along with their values are presented in Table 3.1. This section presents a very brief description of the simulations, their results, and analysis carried out to validate the proposed model [6]. Further analysis of the effect of MAC delays on queuing delays, frame inter-arrival times, and route discovery time was carried out [7–9].

For the network size of N nodes, $(N-2)$ nodes acted as sources and transmitted Constant Bit Rate (CBR) traffic to a common destination node [6]. The destination node acted as a source and transmitted its own packets to another node. In this way, several nodes contended to access the channel leading to collisions and cross-transmissions. A few samples of the network consisting of 10 nodes and 50 nodes are shown in Table 3.2 and Table 3.3, respectively. Certain nodes in the network required

Table 3.3: MAC transmission statistics for a network size of 50 nodes [6]

SID	TTA	BS	CT	$TTBS(ms)$
1	7	0	1	1.724
		1	13	37.894
		2	12	25.784
		3	101	354.198
		4	222	927.126
		5	582	1967.032
		6	73	740.376
2	4	0	14	51.880
		1	4	18.724
		2	78	291.928
		3	297	1241.816
3	3	0	11	49.454
		1	13	50.740
		2	10	40.544

multiple transmission attempts to successfully deliver the packet to their destination [6]. The columns of Table 3.2 indicate the sample ID (SID), the total number of transmission attempts (TTA) for a packet, the backoff stage (BS) of the transmitting node, the number of cross-transmissions (CT) within the backoff stage, and the total time spent in a backoff stage (TTBS). As the network size reached 50 nodes, the retransmission attempts (RETs) reached its threshold. The source nodes that could not deliver their data frames to the destination node aborted further transmissions [6]. The average retransmission count and the average cross-transmissions in the network increased to 5 and 426, respectively. The average packet service-time reached 1956 ms.

Table 3.4 and Figure 3.1 present the details of the network scenarios with various network sizes. The columns of Table 3.4 indicate the network size (NS), the average

Table 3.4: Summary of MAC transmission statistics for different scenarios [6].

NS	ATA	ACT	AC	$ATST(ms)$
10	2.22	15.55	1.22	85.877
20	2.33	34.11	1.33	144.682
30	4.55	167.33	3.55	935.744
40	4.77	372.44	3.77	919.602
50	5.11	426.333	4.11	1956.434

number of transmission attempts (ATA) required for the successful delivery of a frame, the average number of cross-transmissions (ACT) in the network, the average number of collisions (AC) in the network, and the average time required for a successful frame transmission (ATST) in the network [6].

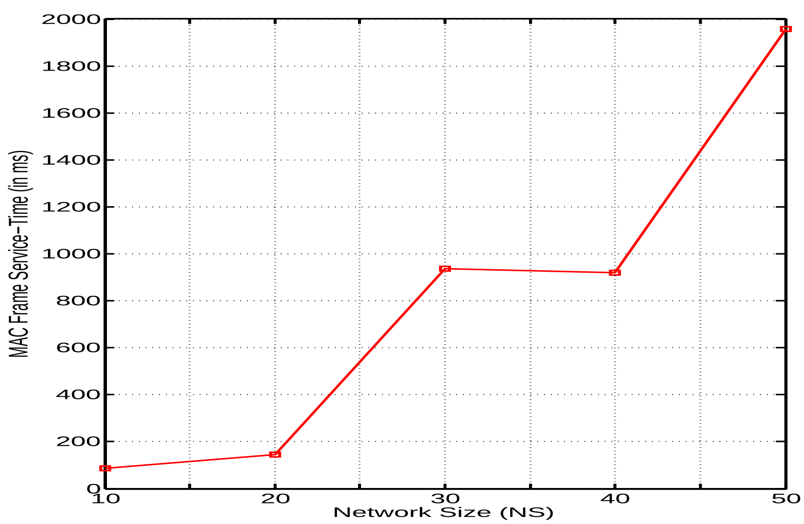

Figure 3.1: Variations in MAC frame service-time because of variations in number of nodes in network.

The simulation results indicate that an increase in the network size increases the

MAC frame service-time, which in-turn effects the node packet service-time [6]. Such pattern of packet service-time can result in high packet end-to-end delays leading to the failure of the real-time applications. Hence, it is essential to reduce the packet transmission delays in ad hoc networks for implementing real-time applications.

3.4 Conclusions

This chapter presented an analytical model for frame service-time in medium access control (MAC) layer and finally the packet service-time at an ad hoc node. This analysis reveals that (a) MAC collisions and cross-transmissions effect the MAC frame service-time in ad hoc networks and they increase with an increase in the network size (number of nodes in the network) and (b) the packet service-time in stationary ad hoc networks primarily depends on MAC frame service-time, whereas in mobile networks it depends on both route discovery time and MAC frame service-time. The MAC frame service-time effected the upper layer delays such as route discovery time associated with the packet transmission process.

This analytical framework is very useful in developing MAC protocols that can reduce the overall delays in the frame transmission process. This research can be extended to analyze the transmission delays of other MAC protocols such as EDCA and their impact on route discovery time and packet service-time in ad hoc networks.

Chapter 4

Semi-Markov Process based Model for the Performance Analysis of Wireless LANs

4.1 Introduction

The MAC delays have a significant impact on packet service-time. Because these delays depend on the specifications of the underlying medium access control (MAC) protocol, the usage of an efficient protocol helps in preventing unnecessary delays in the frame transmission process and increase the network throughput. Hence, it is important to have a well-defined model to analyze the performance of MAC protocols such as the IEEE 802.11 Distributed Coordination Function (DCF) protocol. This chapter presents a semi-Markov process based model for the performance analysis of wireless local area networks (WLANs) employing the IEEE 802.11 DCF protocol.

The two-dimensional Markov chain [10] is used for analyzing the IEEE 802.11 DCF protocol. The two dimensions of this Markov chain represent the backoff stages of the Binary Exponential Backoff (BEB) mechanism and their backoff counters. The state space $|S|$ of the two-dimensional Markov chain is given by [1, 10]

$$|S| = \sum_{i=0}^{m} 2^i CW_{min} = CW_{min}(2^{m+1} - 1) \tag{4.1.1}$$

where i represents the backoff stage of the BEB mechanism, m represents the highest backoff stage, and CW_{min} represents the minimum contention window. For the Frequency Hopping Spread Spectrum (FHSS) physical layer specifications, the state space $|S|$ of the Markov chain is [1]

$$|S| = 16 \times (2^7 - 1) = 2032 \tag{4.1.2}$$

The state space of the two-dimensional Markov chain is very large in the order $O(2^m)$ [1]. A new model with reduced state space is proposed which computes (without compromising the accuracy) the wireless network parameters such as conditional collision probability, node's packet transmission probability, and saturation throughput in the wireless LAN [1].

4.2 Modeling the BEB Mechanism Using the Semi-Markov Process

In this section, the BEB mechanism is modeled using the semi-Markov process [1]. In subsection 4.2.1, an (m+1)-state Markov chain is constructed to describe the backoff stages of the BEB mechanism. Because the backoff intervals associated with different backoff stages of the BEB mechanism are not equal, this discrete-time Markov chain with a unit state holding time for all its states cannot completely describe the BEB mechanism. So, an embedded Markov chain is constructed in subsection 4.2.2 that allows different state holding times for its states. However, this embedded Markov chain does not include self-loops (transition from state i to itself). In subsection 4.2.3, the backoff intervals of backoff stages of the BEB mechanism are modeled as state holding times of the semi-Markov process which allows self-loops and, also, different state holding times for its states. Also, we compute the stationary probabilities for the semi-Markov process. Subsection 4.2.4 computes the parameters of interest (including saturation throughput) based on the proposed model.

4.2.1 Construction of (m+1)-state Markov Chain

The (m+1)-states of the Markov chain in Figure 4.1 represent the backoff stages of the BEB mechanism of the IEEE 802.11 DCF MAC protocol [1]. The node performs its first packet transmission while it is in state zero.

If the transmission is successful, it loops back to the same state and initiates the next packet transmission. In the event of collision, the node proceeds for a retransmission and enters the backoff stage one represented by state one. If the packet collides again, the node transitions to the next backoff stage represented by state two for the retransmission. These state transitions continue until the packet is successfully transmitted, or the node reaches the highest backoff stage m. When the node reaches the backoff stage m, it returns to the same backoff stage for retransmissions after collisions. Once the packet transmission count reaches the threshold value, the packet is dropped and a new packet is served. In summary, any state i of the semi-Markov process represents the i^{th} backoff stage of the BEB mechanism. The transition from a lower state i to a higher state $(i + 1)$ indicates an unsuccessful transmission. The transition from any state i to state 0 indicates a successful transmission. The loopback transitions are possible only for states 0 and m.

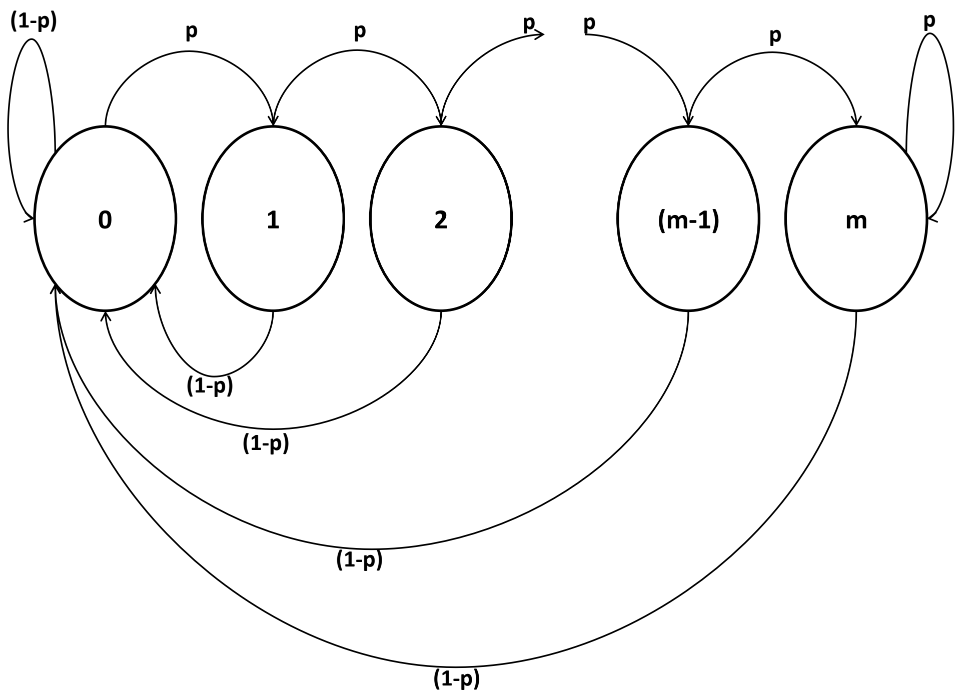

Figure 4.1: (m+1)-state Markov chain with state transition probabilities $P_{i,(i+1)}$ representing the transition from state i to $(i+1)$ [1].

The state transitions of the (m+1)-state Markov chain are represented by the state transition probability matrix $[\mathbf{P}]$ given by [1, 10, 32]

$$[\mathbf{P}] = \begin{pmatrix} (1-p) & p & 0 & \cdots & 0 \\ (1-p) & 0 & p & \cdots & 0 \\ (1-p) & 0 & 0 & \cdots & 0 \\ \cdot & \cdot & \cdot & \cdot & \cdot \\ (1-p) & 0 & 0 & \cdots & p \\ (1-p) & 0 & 0 & \cdots & p \end{pmatrix} \tag{4.2.1}$$

where $P_{(i-1)i}$, $0 \leq i < m$, is the probability of transition from state i to state $(i+1)$, and is equal to *conditional collision probability* p defined as [1,10]

$$p = 1 - (1 - \tau)^{(N-1)} \tag{4.2.2}$$

where τ is the node's packet transmission probability, and N is the number of nodes in the saturated local area network (LAN). The key assumption considered here regarding p is the same as the assumption of [1] constant and independent collision

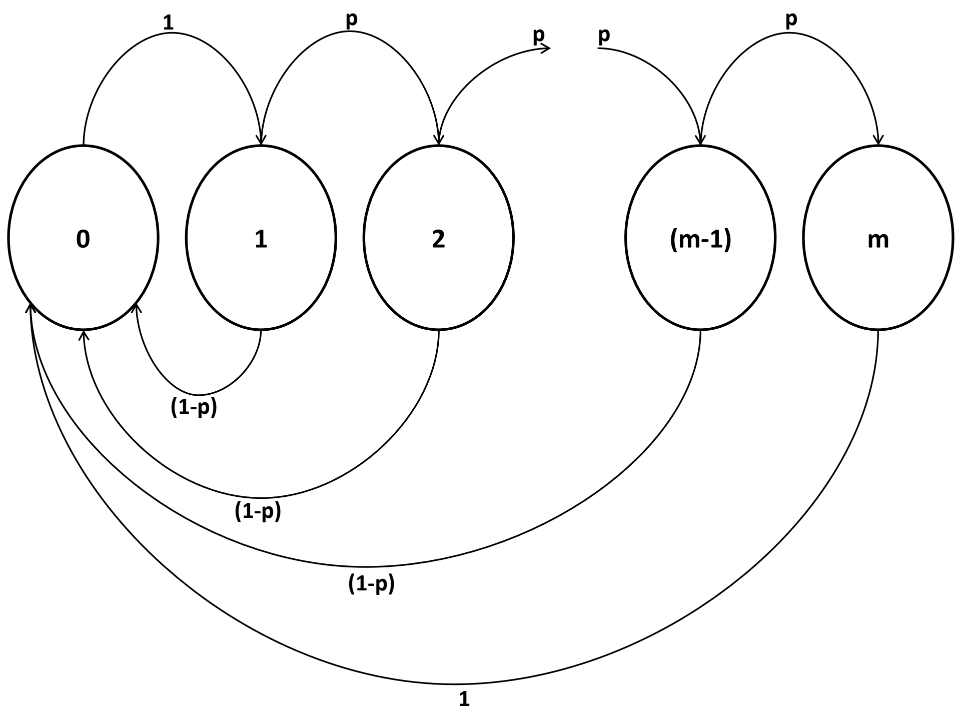

Figure 4.2: (m+1)-state embedded Markov chain with $P^e_{ii} = 0$.

probability of a packet transmitted by each station, regardless of the number of retransmissions already suffered [1,10].

4.2.2 Construction of (m+1)-state Embedded MC

In this subsection, the Markov chain presented in Figure 4.1 is transformed into an embedded Markov chain (with $P_{ii} = 0 \, \forall$ i), as shown in Figure 4.2 [1]. The element P^e_{ij} of the state transition probability matrix $[\mathbf{P}]^e$ of an embedded Markov chain is [1,32]

$$
\begin{aligned}
P^e_{ij} &= \quad 0 \qquad for\ i = j &(4.2.3)\\
&= \frac{P_{ij}}{(1 - P_{ii})}\ for\ i \neq j &(4.2.4)
\end{aligned}
$$

which results in

$$
[\mathbf{P}]^e = \begin{pmatrix} 0 & 1 & 0 & \cdots & 0 \\ (1-p) & 0 & p & \cdots & 0 \\ (1-p) & 0 & 0 & \cdots & 0 \\ . & . & . & . & . \\ (1-p) & 0 & 0 & \cdots & p \\ 1 & 0 & 0 & \cdots & 0 \end{pmatrix} \tag{4.2.5}
$$

The stationary probability Π^e_i of state i of the embedded Markov chain is given by [1,32]

$$
\Pi^e_i = \sum_{j \neq i} \Pi^e_j P^e_{ji}, \qquad \forall\ i\ \in\ (0, m) \tag{4.2.6}
$$

This yields the following set of simultaneous equations [1]

$$
\begin{aligned}
\Pi^e_0 &= \Pi^e_1 P^e_{10} + \Pi^e_2 P^e_{20} + \Pi^e_3 P^e_{30} + \cdots + \Pi^e_m P^e_{m0} \\
\Pi^e_1 &= \Pi^e_0 P^e_{01} + \Pi^e_2 P^e_{21} + \Pi^e_3 P^e_{31} + \cdots + \Pi^e_m P^e_{m1} \\
\Pi^e_i &= \Pi^e_0 P^e_{0i} + \Pi^e_1 P^e_{1i} + \cdots + \Pi^e_{(i-1)} P^e_{(i-1)i} + \Pi^e_{(i+1)} P^e_{(i+1)i} + \cdots + \Pi^e_m P^e_{m2} \\
\Pi^e_{m-1} &= \Pi^e_0 P^e_{0(m-1)} + \Pi^e_1 P^e_{1(m-1)} + \Pi^e_2 P^e_{2(m-1)} + \cdots + \Pi^e_{(m-2)} P^e_{(m-2)(m-1)} + \Pi^e_m P^e_{m(m-1)} \\
\Pi^e_m &= \Pi^e_0 P^e_{0m} + \Pi^e_1 P^e_{1m} + \Pi^e_2 P^e_{2m} + \cdots + \Pi^e_{(m-1)} P^e_{(m-1)m}
\end{aligned}
$$

Substituting the state transition probabilities P_{ij}^e obtained from $[\mathbf{P}]^e$ in the simultaneous equations, we have [1]

$$\begin{aligned}
\Pi_0^e &= \{\Pi_1^e \times (1-p)\} + \{\Pi_2^e \times (1-p)\} + \{\Pi_3^e \times (1-p)\} + \cdots + \Pi_m^e \\
\Rightarrow \Pi_0^e &= (1-p)\{\Pi_1^e + \Pi_2^e + \Pi_3^e + \cdots + \Pi_{(m-1)}^e\} + \Pi_m^e \\
\Pi_1^e &= \{\Pi_0^e \times 1\} + \{\Pi_2^e \times 0\} + \{\Pi_3^e \times 0\} + \cdots + \{\Pi_m^e \times 0\} \\
\Rightarrow \Pi_1^e &= \Pi_0^e \\
\Pi_i^e &= \Pi_0^e \times p^{i-1} \\
\Pi_{m-1}^e &= \Pi_0^e \times p^{(m-2)} \\
\Pi_m^e &= \Pi_0^e \times p^{(m-1)}
\end{aligned}$$

Also

$$\Pi_0^e + \Pi_1^e + \Pi_2^e + \Pi_3^e + \cdots + \Pi_m^e = 1$$

Solving these simultaneous equations, we obtain the stationary probabilities of the embedded Markov chain as [1]

$$\begin{aligned}
\Pi_0^e &= \frac{(1-p)}{(2-p-p^m)} \\
\Pi_1^e &= \frac{(1-p)}{(2-p-p^m)} \\
\Pi_i^e &= \frac{(1-p)p^{i-1}}{(2-p-p^m)} \\
\Pi_{m-1}^e &= \frac{(1-p)p^{(m-2)}}{(2-p-p^m)} \\
\Pi_m^e &= \frac{(1-p)p^{(m-1)}}{(2-p-p^m)}
\end{aligned}$$

which can be summarized as [1]

$$\Pi_0^e = \Pi_1^e = \frac{(1-p)}{(2-p-p^m)} \tag{4.2.7}$$

$$\Pi_i^e = \frac{(1-p)p^{i-1}}{(2-p-p^m)}, \ \forall \ i \ \in \ (2, m) \tag{4.2.8}$$

which constitute the stationary probability vector Π^e represented as $[\Pi_0^e \, \Pi_1^e \, \Pi_2^e \, \ldots \, \Pi_m^e]$.

4.2.3 Stationary Probabilities of the Semi-Markov Process

Stationary probability Π_i^s of state i of the semi-Markov process is [1, 32]

$$\Pi_i^s = \frac{\Pi_i^e \times E[H_i]}{\sum_{j=0}^{m}\{\Pi_j^e \times E[H_j]\}}, \ 0 \leq i \leq m \tag{4.2.9}$$

The state holding time H_i is defined as the time-period for which the node remains in a particular state i before transition to another state [32]. In this subsection, the backoff interval of backoff stage i is modeled as the state holding time for state i in the Markov chain. The state holding time for state i is a random variable selected uniformly within the range $(0, 2^i CW_{min})$, for $0 \leq i \leq m$ [1].

The expected value of state the holding-time $E[H_i]$ for state i of the semi-Markov process is given by [1]

$$\begin{aligned} E[H_i] &= \frac{2^i CW_{min}}{2}, \qquad 0 \leq i \leq m \\ &= 2^{i-1} CW_{min} \end{aligned} \tag{4.2.10}$$

As the node visits state 0 and state m successively after a successful transmission in backoff stage 0 and collision in backoff stage m, respectively, the expected number of consecutive visits to states 0 and m equal $\frac{1}{p}$ and $\frac{1}{(1-p)}$, respectively [1]. Hence, the expected value of state holding time for states 0 and m are [1]

$$E[H_0] = \frac{2^0 CW_{min}}{2} \times \frac{1}{p} = \frac{CW_{min}}{2p} \tag{4.2.11}$$

$$E[H_m] = \frac{2^m CW_{min}}{2} \times \frac{1}{(1-p)} = \frac{2^{m-1} CW_{min}}{(1-p)} \tag{4.2.12}$$

Using (4.2.9) and $\sum_{i=0}^{m} \Pi_i^s = 1$, the stationary probabilities of the semi-Markov process are derived as [1]

$$\begin{aligned}
\Pi_0^s &= \frac{\frac{1}{2p}}{\frac{CW_{min}}{2p} + \sum_{j=1}^{m-1}\{\Pi_j^e * 2^{j-1} CW_{min}\} + \frac{2^{m-1}CW_{min}}{(1-p)}} \\
\Pi_1^s &= \frac{1}{\frac{CW_{min}}{2p} + \sum_{j=1}^{m-1}\{\Pi_j^e * 2^{j-1} CW_{min}\} + \frac{2^{m-1}CW_{min}}{(1-p)}} \\
\Pi_i^s &= \frac{(2p)^{i-1}}{\frac{CW_{min}}{2p} + \sum_{j=1}^{m-1}\{\Pi_j^e * 2^{j-1} CW_{min}\} + \frac{2^{m-1}CW_{min}}{(1-p)}}, \quad i \in (1, m-1) \\
\Pi_m^s &= \frac{\frac{(2p)^{m-1}}{(1-p)}}{\frac{CW_{min}}{2p} + \sum_{j=1}^{m-1}\{\Pi_j^e * 2^{j-1} CW_{min}\} + \frac{2^{m-1}CW_{min}}{(1-p)}}
\end{aligned}$$

Stationary probability Π_i^s of the semi-Markov process represents the fraction of time spent by a node in backoff stage i.

4.2.4 Node Packet Transmission Probability and Saturation Throughput of the Channel

Next, the stationary probability distribution of the semi-Markov process and the state holding times are used to compute the saturation throughput in the network [1]. The packet transmission probability τ is calculated as follows. If the system is in state i, the node transmits once after an expected time interval $E[H_i]$, for $0 \leq i \leq m$ [1]. In state 0, the node transmits once after an expected time interval of $E[H_0]/(1/p)$. Similarly, the average time interval before transmission is computed for state m. Thus,

τ can be expressed as [1]

$$
\begin{aligned}
\tau &= \frac{\Pi_0^s(\frac{1}{p})}{E[H_0]} + \frac{\Pi_1^s}{E[H_1]} + \frac{\Pi_2^s}{E[H_2]} + \ldots + \frac{\Pi_m^s(\frac{1}{1-p})}{E[H_m]} \\
&= \frac{\frac{1-p}{2-p-p^m}\left\{\frac{1}{p} + \sum_{j=0}^{m-2}(p)^j + \frac{p^{m-1}}{1-p}\right\}}{\frac{(1-p)CW_{min}}{2-p-p^m}\left\{\frac{1}{2p} + \sum_{j=0}^{m-2}(2p)^j + \frac{(2p)^{m-1}}{1-p}\right\}} \\
&= \frac{\left\{\frac{1}{p} + \sum_{j=0}^{m-2}(p)^j + \frac{p^{m-1}}{1-p}\right\}}{CW_{min}\left\{\frac{1}{2p} + \sum_{j=0}^{m-2}(2p)^j + \frac{(2p)^{m-1}}{1-p}\right\}} \qquad (4.2.13)
\end{aligned}
$$

The saturation throughput S of the channel is [1, 10]

$$
S = \frac{P_s P_{tr} E[P]}{(1 - P_{tr})\rho + P_{tr} P_s T_s + P_{tr}(1 - P_s)T_c} \qquad (4.2.14)
$$

where P_{tr} is the probability of a node transmitting a packet, P_s is the probability of successful transmission, ρ is the idle slot time, T_s is the average time spent in a successful transmission, and T_c is the average time spent in collisions. These parameters are defined as [10]

$$
\begin{aligned}
P_{tr} &= 1 - (1 - \tau)^N \qquad (4.2.15) \\
P_s &= \frac{N\tau(1 - \tau)^{(N-1)}}{1 - (1 - \tau)^N} \qquad (4.2.16) \\
T_s^{rts} &= DIFS + RTS + CTS + Hdr \\
&+ E[P] + ACK + 3SIFS + 4\mu \qquad (4.2.17) \\
T_c^{rts} &= DIFS + RTS + \mu \qquad (4.2.18)
\end{aligned}
$$

The value τ given by (4.2.13) is used in the above computation. $DIFS$ represents the distributed inter-frame space, RTS is the time spent for RTS transmission, CTS is the time spent for CTS transmission, Hdr is the sum of MAC and physical layer headers, $E[P]$ is the average payload, ACK is the time spent for ACK transmission, $SIFS$ is the short inter-frame space, and δ is the propagation delay.

4.3 The Evaluation of Proposed Model

The Matlab evaluation was carried out: (a) to compute the essential network parameters ($\tau_S,\ p_S,\ and\ S_S$) of wireless networks using the proposed model [1], and (b) to evaluate the computation time for the proposed semi-Markov process [1]. The results were validated by comparing them with those from Bianchi's model [1,10]. τ_B denotes the value of τ obtained using Bianchi's analysis, and τ_S denotes the value of τ obtained using the proposed model (4.2.13) [1].

For (a): The conditional collision probability (p_S) and packet transmission probability (τ_S) were computed using (4.2.2) and (4.2.13) for a fixed number of nodes, using fixed point iteration method. These outputs were further used for computing the saturation throughput of the channel using (4.2.14) through (4.2.18). Table 4.1 presents various parameters and their values used for computing saturation throughput (S_S) [1]. These computations were performed for different values of N for fixed

Table 4.1: FHSS system parameters used for computing saturation throughput [10]

$Parameter$	$Value$
$E[P]$	8184 $bits$
$MAC\ header$	272 $bits$
$PHY\ header$	128 $bits$
ACK	112 $bits + PHY\ header$
RTS	160 $bits + PHY\ header$
CTS	112 $bits + PHY\ header$
$Channel\ Bit\ Rate$	1 $Mbits/s$
$Propagation\ Delay$	1 μs
$Slot\ Time$	50 μs
$SIFS$	28 μs
$DIFS$	128 μs

values of $m = 3$ and $CW_{min} = 32$, and the results obtained were compared with those from Bianchi's model ($\tau_B,\ p_B,\ and\ S_B$). The outputs obtained for both models are presented in Table 4.2. Furthermore, the saturation throughputs S_B and S_S are compared for the variations in CW_{min} (from 8 through 1024), and these results are presented in Table 4.3. The saturation throughput obtained using the proposed

Table 4.2: Comparison of ($\tau_B,\ p_B,\ S_B$) and ($\tau_S,\ p_S,\ S_S$) for variations in N; for constant m and CW_{min} of 3 and 32, respectively. [1]

N	(τ_B, p_B, S_B)	(τ_S, p_S, S_S)
2	(0.0570, 0.0570, 0.8189)	(0.0586, 0.0586, 0.8198)
3	(0.0538, 0.1046, 0.8279)	(0.0551, 0.1071, 0.8284)
5	(0.0481, 0.1794, 0.8343)	(0.0491, 0.1823, 0.8345)
10	(0.0387, 0.2986, 0.8371)	(0.0392, 0.3024, 0.8371)
15	(0.0329, 0.3750, 0.8367)	(0.0333, 0.3770, 0.8366)
20	(0.0291, 0.4302, 0.8356)	(0.0293, 0.4328, 0.8355)
30	(0.0242, 0.5078, 0.8329)	(0.0243, 0.5116, 0.8327)
40	(0.0212, 0.5644, 0.8300)	(0.0213, 0.5665, 0.8299)
50	(0.0190, 0.6104, 0.8269)	(0.0191, 0.6123, 0.8268)
60	(0.0174, 0.6467, 0.8240)	(0.0175, 0.6483, 0.8238)
70	(0.0162, 0.6772, 0.8209)	(0.0162, 0.6788, 0.8208)
80	(0.0153, 0.7012, 0.8182)	(0.0152, 0.7050, 0.8177)
90	(0.0144, 0.7266, 0.8148)	(0.0145, 0.7256, 0.8149)
100	(0.0137, 0.7470, 0.8116)	(0.0137, 0.7485, 0.8113)
150	(0.0115, 0.8233, 0.7944)	(0.0115, 0.8244, 0.7941)

model was observed to be fairly accurate compared with that obtained using the Bianchi's model for all values of N and CW_{min}.

For (b): The computation times needed to solve for the saturation throughput under both models for various values of N presented in Table 4.2 were compared. The computation time includes the time needed to solve for the stationary probability distribution, and fixed point equations for τ and p. These results are presented in Table 4.4. The simulations show that the proposed model requires one-tenth of the

Table 4.3: Comparison of (τ_B, p_B, S_B) and (τ_S, p_S, S_S) for variations in CW_{min}; for constant m and N of 3 and 100, respectively. [1]

CW_{min}	(τ_B, p_B, S_B)	(τ_S, p_S, S_S)
8	(0.0331, 0.9647, 0.6496)	(0.0336, 0.9662, 0.6436)
16	(0.0205, 0.8720, 0.7749)	(0.0206, 0.8738, 0.7740)
32	(0.0137, 0.7470, 0.8116)	(0.0137, 0.7485, 0.8113)
64	(0.0095, 0.6134, 0.8267)	(0.0095, 0.6142, 0.8266)
128	(0.0066, 0.4761, 0.8339)	(0.0066, 0.4765, 0.8339)
256	(0.0044, 0.3558, 0.8362)	(0.0044, 0.3563, 0.8362)
512	(0.0028, 0.2367, 0.8340)	(0.0028, 0.2368, 0.8340)
1024	(0.0016, 0.1459, 0.8253)	(0.0016, 0.1460, 0.8253)

time required for computing the stationary probabilities using Bianchi's model.

4.3.1 Results and Discussion

This subsection presents the analysis of results presented in Tables 4.2 and 4.4 [1].

1. *Output Parameters*: The simulation results presented in Table 4.2 show that the outputs of the proposed model are close to those of Bianchi's model with a maximum difference of 0.1 percent for the saturation throughput S [1]. An increase in N results in an increase in p and a decrease in τ for both models. For $N = 2$, the values of p and τ are equal according to (4.2.2). With an increase in N, the saturation throughput increased until the channel throughput reached its maximum value. With the further increase in the number of network nodes, the saturation throughput reduces and reaches zero as $N \to \infty$. This pattern is visible in the outputs of the proposed model as also seen from the Bianchi's model from Table 4.2. The saturation throughput reached its peak very close to 84 percent at $N = 10$ in both cases validating the accuracy of the proposed

Table 4.4: Comparison of computational time for Bianchi's model (C_B) and the proposed model (C_S) [1]

N	C_B (in ms)	C_S (in ms)
2	1.3ms	0.10174ms
3	0.77390ms	0.081299ms
5	0.78945ms	0.082632ms
10	0.83832ms	0.079522ms
15	0.82677ms	0.099070ms
20	0.80233ms	0.098626ms
30	0.79434ms	0.080855ms
40	0.79567ms	0.082632ms
50	0.79389ms	0.095960ms
60	0.80811ms	0.082188ms
70	0.79922ms	0.081299ms
80	0.77657ms	0.081744ms
90	0.80278ms	0.084409ms
100	0.79789ms	0.082181ms
150	0.82188ms	0.083077ms

model. Figures 4.3 and 4.4 present the variations of p, τ, and S with respect to N for both Bianchi's model and the proposed model, and also with respect to CW_{min} for a constant N of 100.

2. *Computation Time*: The Matlab implementation of the two models shows that the proposed model requires one-tenth of the time required for implementing (computing the stationary probabilities of) Bianchi's model [1]. The computation time is obtained using the Matlab commands *tic* and *toc*. Table 4.4 presents the computation time for the two models for variations in N. The computation time is almost constant for both models for variations in N [1].

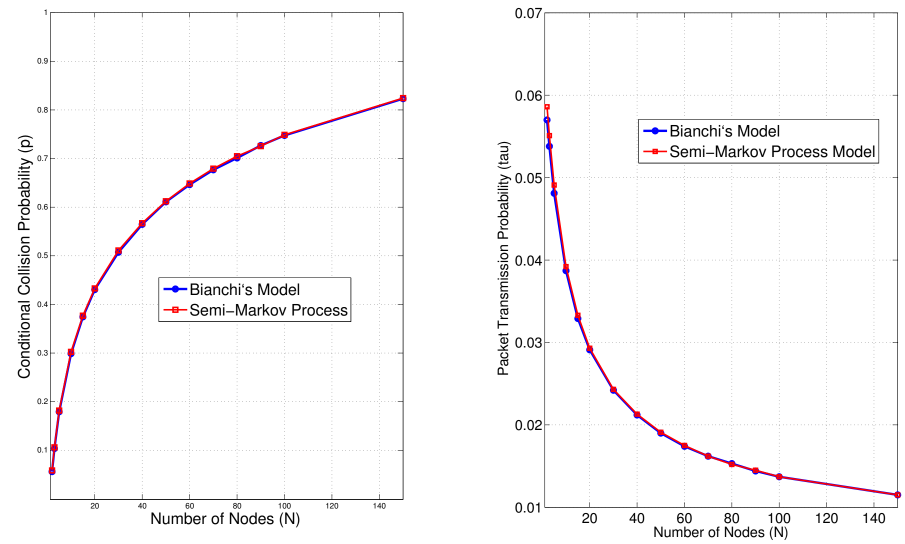

Figure 4.3: (a) Variations of condition collision probability with number of network nodes [1]. (b) Variations in packet transmission probability with number of network nodes [1].

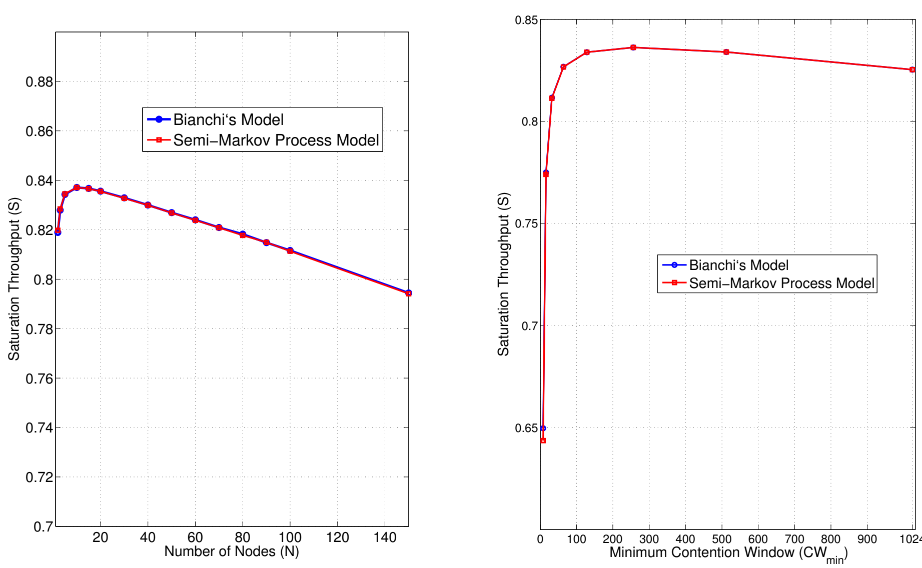

Figure 4.4: (a) Variations of saturation throughput with number of nodes [1]. (b) Variations of saturation throughput with minimum contention window [1].

4.4 Conclusions

In this chapter, the Binary Exponential Backoff (BEB) mechanism of the IEEE 802.11 DCF protocol was modeled using the semi-Markov process [1]. Various backoff stages of the BEB mechanism and their backoff counters were modeled as the state of the semi-Markov process and their state holding times, thus reducing the two-dimensional Markov chain to a one-dimensional process. Unlike the two-dimensional Markov chain with an order of $O(2^m)$ states, the semi-Markov process has very few states of order $O(m)$. The proposed model presents a new and simpler approach to compute the essential parameters such as conditional collision probability, packet transmission probability, and saturation throughput without compromising the accuracy. The Matlab evaluation of the proposed semi-Markov process shows that it requires one-tenth of the time required for computing the same network parameters of interest using Bianchi's two-dimensional Markov chain model. Thus, the proposed model achieves accurate results close to those of Bianchi's model with less complexity and computation time, and hence is more suitable towards analyzing sophisticated protocols such as the IEEE 802.11e with EDCA [1].

Chapter 5

Literature Survey on Burst Loss Models in VoIP

5.1 Introduction

This chapter presents the literature survey on burst losses models in Voice over Internet Protocol (VoIP) in three sections followed by an outline of the research work presented in chapter six.

5.2 Analytical Models

This section describes research issues such as the packet arrival process and the packet loss in VoIP analysis. Bolot [33] used the round-trip delay of User Datagram Protocol (UDP) packets for characterizing end-to-end packet delay and loss behavior over the Internet. He studied the structure of the Internet load by varying the interval between probe packets. The time scales considered for this study ranged from a few milliseconds to a few minutes. Their experimental results matched simulation results of other researchers. The inter-arrival time for the Internet packets was observed to follow exponential distribution. Also, the losses were found to be random, given that the probe traffic consumed a small fraction of the available bandwidth. Later, Bolot et al. [34] analyzed the problem of voice packet drops over the network that do not provide any support for the real-time applications. Voice quality was observed to be mediocre due to the large number of packet losses. Also, random losses were observed under low and moderate load conditions. The authors concluded that the lost packets can be reconstructed using an open-loop error-control mechanism based on the principle of FEC. Borella [35] conducted several experiments to obtain Internet packet-loss traces for speech transmission over three different Internet paths. Burst losses were modeled using Pareto distribution, and their dependency and predictability were analyzed using the concept of conditional entropy. Several parameters such as client-to-server loss rate, server-to-client loss rate, and round-trip loss rate were used in this analysis. Asymmetry of packet loss over various paths was also discussed.

Kaj and Marsh [36] modeled the delay variations of audio packets arriving at the receiver in VoIP systems. The primary emphasis of this work is to identify and model the effect of certain network layer delays (such as queuing delay), packet loss and silence suppression (at the sender) on the overall packet end-to-end delay, and the packet arrival times at the receiver. The authors initially modeled the packet queuing delays and packet transmission delays at various routers on the path from source to destination. Furthermore, they claim that the packet end-to-end delays form a Markov chain. This packet end-to-end delay is assumed to be the time gap between its transmission at the sender, and its arrival time at the receiver. In addition, the delays caused by (a) silence suppression at the sender, and (b) tracking of lost packets and re-ordering of non-lost packets are modeled along with their impact on the packet arrival pattern at receiver.

Pragtong et al. [37] model the real-time VoIP traffic in terms of talkspurts and silent durations. They proposed a new conversational model based on the measured data of the packet switched networks of ToT Public Company Limited (Plc) located in Thailand. They primarily analyzed the effect of background noise and ring tones on the model. For this, they proposed an addition of a new state, known as the long burst, into the existing model to represent background noise at the sender's place. From the information obtained from the IP network of the ToT Plc, the authors noticed that the long bursts increased the data rate of VoIP traffic by 60 percent. Biernacki [38] modeled the VoIP gateway as a VoIP traffic multiplexor and analyzed its performance. The multiplexor received the input packets from several independent sources, and is assumed to possess an output link with a fixed data rate. Koutras and Platis [39] studied the resource allocation aspects of a VoIP network. They modeled the resource allocation process in the VoIP networks and discussed the resource degradation caused by the increasing demands for resources in these networks. The authors proposed software rejuvenation for increasing the availability and reliability of the network resources for VoIP calls, and modeled the software rejuvenation as a semi-Markov process.

Lu et al. [40] analyzed the packet loss in ad hoc networks through simulations. Their simulation results reveal that the packet loss in stationary ad hoc networks is caused by queue congestion, and that in mobile ad hoc networks is caused by route unavailability and queue congestion. Also, the packet loss in mobile network occurs at both the source and intermediate nodes.

5.3 Packet Loss Models Based on Markov Chains

Very few VoIP models took packet loss into account. Many existing models were based on Markov chains such as the Gilbert model (2-state Markov model),the m^{th}-order Markov model, and the extended Gilbert model. None of these models considered inter-arrival time of the voice packets as an important parameter that contributes to burst losses.

The Gilbert model uses a Markov chain with two states, namely (1) and (0), representing a loss state and a no-loss state, respectively. The network enters the loss state (1) if a packet is dropped; otherwise, it enters a no-loss state (0). Transition probabilities are determined by taking the number of losses into consideration. Once these transition probabilities are defined and the state transition probability matrix is formed, the state of the network at any given instant can be determined. Finally, the limiting state probability vector shows the state of the network at the equilibrium condition (time tending to infinity).

The m^{th}-order Markov model takes into consideration the last m events to decide the future. It needs 2^m states to predict the next state. Although it captures burst losses, it is a very complicated model and needs a very large number of parameters to be calculated.

The extended Gilbert model needs only $(m + 1)$ states to remember the past m events. Other than 0, there are m states in this model. A randomly selected state i represents i consecutive losses. Depending on the present state, the queue decides the next state. The Gilbert model is a special case of the extended Gilbert model.

All calculations in the Gilbert model are applicable to the extended Gilbert model, including a state transition probability matrix, an initial state probability vector, and a limiting state probability vector. Of importance with the extended Gilbert model is that the queue can make a transition from state i to either $(i+1)$ or 0. Other than these, no other transitions are possible. However, if i is equal to 0, then this rule does not apply. That is, the network can make an immediate transition back to state 0 if it was previously in that state, or it can jump to state 1.

Yagnik et al. [41] presented a detailed analysis of 128-hour end-to-end unicast and multicast packet-loss measurements. Using these traces, the authors evaluated the accuracy of three different models of increasing complexity in capturing the temporal dependency of the packet loss. The models used in the analysis were the Bernoulli model, the 2-state Markov chain model, and the k-th order Markov chain model. The packet-loss traces were obtained by transmitting unicast and multicast packet probes at periodic intervals of 20ms, 40ms, 80ms, and 160ms, and recording the sequence numbers of the packets successfully received at the destination. It was observed that the estimated order of the Markov chain model (value of k) ranged from 10 to 42. Sanneck and Carle [42] analyzed the temporal dependency of packet loss using Markov models of varying complexity. They presented an analytical framework for a comprehensive characterization of packet loss process. The framework provides four important models that are applicable to four different cases of packet loss: an infinite number of consecutive losses, a finite number of consecutive losses, a special case of a system having the memory of a single (previous) packet, and a finite number of successful transmissions. These models aimed at capturing burst losses and the distance between them. In the first two cases, the Markov chain had $(m+1)$ states.

The value of m tends to infinity in the first case, whereas in the second case, it is a finite number that is suited to real-time applications such as voice and video. Model parameters are derived from the run lengths of received and lost packets. The authors conclude that real-time applications required an intermediate model that is more complex than the simple Gilbert model.

Jiang and Schulzrinne [43] modeled the delay and packet loss in a VoIP system and the correlation between them. They also proposed joint use of the extended Gilbert model and the inter-loss distance (ILD) metric for analyzing and characterizing the temporal dependency of the packet loss [44]. In addition, they proposed a new metric called the Conditional Cumulative Distributive Function (CCDF) for measuring delay. The effectiveness of the model is evaluated based on the final loss pattern obtained after the application of playout delay adjustment and Forward Error Correction (FEC) techniques. Sanneck et al. [45] modeled packet-loss distribution within a voice flow using a 2-state Markov chain and a $(m + 1)$-state Markov chain to define the objective speech quality metrics. These metrics were later used in the study of codecs and related algorithms. Frost [46] proposed a metric for characterizing network congestion in terms of QoS observed by an end user. He also proposed a mechanism for predicting the rate of congestion events, which gives the average time gap between any two successive congestion events. The metric proposed by Frost is similar to the ILD metric.

5.4 Extended Gilbert Model

This subsection discusses the extended Gilbert model proposed by Sanneck [42]. Figure 5.1 presents the state diagram of the (m+1)-state extended Gilbert model [42].

State 0 represents a no-loss state and states 1 through m represent lossy states. In

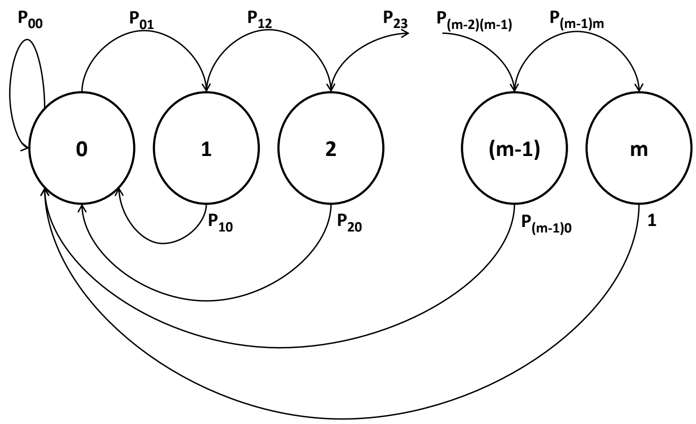

Figure 5.1: Extended Gilbert model consisting of $(m+1)$ states. P_{ij} represents the state transition probability from state i to j.

other words, the burst loss state i represents the loss of i consecutive packets. The maximum number of consecutive losses is bound by a finite value of m [42].

Every time a voice packet arrives at the Internet router queue, it is either dropped or accommodated into the queue, depending on the queue status. When the burst loss state is i where $0 \leq i < m$, if the incoming packet is accepted then burst loss state becomes 0; else it becomes $(i+1)$. The burst loss state reaches its limit when it reaches m, and the burst loss count is reset to zero at the next arrival. This causes the transition probability P_{m0} from state m to state 0 to be 1 after m consecutive losses. It may be noted that the self-loops are allowed only for state 0 in the Discrete-Time Markov Chain (DTMC) of the extended Gilbert model.

The state transition probability matrix $[\mathbf{P}]$ for the extended Gilbert model is described by [42, 44]

$$[\mathbf{P}] = \begin{pmatrix} P_{00} & P_{01} & 0 & \cdot & 0 \\ P_{10} & 0 & P_{12} & \cdot & 0 \\ P_{20} & 0 & 0 & \cdot & 0 \\ \cdot & \cdot & \cdot & \cdot & \cdot \\ P_{(m-1)0} & 0 & 0 & \cdot & P_{(m-1)m} \\ 1 & 0 & 0 & \cdot & 0 \end{pmatrix} \quad (5.4.1)$$

where $P_{(i-1)i}$ is the probability of the transition of the burst loss state from $(i-1)$ to i, and it is given by the ratio of number of transitions $V_{(i-1)}$ from state $(i-2)$ to $(i-1)$ to the number of transitions (V_i) from state $(i-1)$ to state i, $0 \leq i < m$.

$$P_{(i-1)i} = \frac{V_i}{V_{i-1}} \quad (5.4.2)$$

Suppose that the state transition probability $P_{(i-1)i}$ and $P_{(i-1)0}$ are represented as $a_{(i-1)}$ and $(1 - a_{(i-1)})$. Then,

$$[\mathbf{P}] = \begin{pmatrix} (1-a_0) & a_0 & 0 & \cdots & 0 \\ (1-a_1) & 0 & a_1 & \cdots & 0 \\ (1-a_2) & 0 & 0 & \cdots & 0 \\ \cdot & \cdot & \cdot & \cdot & \cdot \\ (1-a_{m-1}) & 0 & 0 & \cdots & a_{m-1} \\ 1 & 0 & 0 & \cdots & 0 \end{pmatrix} \quad (5.4.3)$$

The stationary probabilities of the $(m+1)$-state Markov chain are obtained as n tends to ∞ in the following equation [47].

$$\Pi^n = \Pi^0 \times [\mathbf{P}]^n \quad (5.4.4)$$

where Π^0 represents the initial state probability vector, Π_i^0 represents the i^{th} element of Π^0, and Π_i^n represents the i^{th} element of Π^n.

The above discussion reveals that the burst losses in VoIP were previously analyzed using empirical models based on the Markov chains. The extended Gilbert model, which was the latest model used for analyzing the burst losses, assumes that all the incoming packets arrive at the queue with a unit packet inter-arrival times. However, packets arrive at an Internet router with varying inter-arrival times; and it may not be appropriate to generalize that the inter-arrival times of all packets are same. Therefore, the inclusion of a time parameter such as state holding time explains the burst loss patterns more accurately. It helps in capturing the state transitions and the time intervals between them in the extended Gilbert model. This requirement of a time parameter to model the packet inter-arrival time is fulfilled in the model discussed in chapter six.

Chapter 6

Analysis of Burst Losses in IP Networks Using the Semi-Markov Process

6.1 Introduction

Burst losses severely degrade the quality of real-time applications on the Internet, such as Voice over Internet Protocol (VoIP) [2]. When several consecutive packets of a particular voice flow are dropped, the voice codecs at the destination fail to interpolate the lost packets from the available voice datagrams. It may not be possible for a loss concealment algorithm to completely compensate the effect of burst losses on voice quality [44]. Therefore, in order to minimize such losses it is very important to understand the primary cause of burst losses. The variations in packet inter-arrival times effect the packet drops at the router queue with a constant packet service-rate and fixed capacity. The low packet inter-arrival times result in burst losses. In this chapter, burst losses in VoIP are modeled as a semi-Markov process by incorporating packet inter-arrival time in the extended Gilbert model described in the previous chapter. The relationship between the packet inter-arrival time and burst losses is developed in terms of stationary probabilities of semi-Markov process as described in the following section.

6.2 The Proposed Semi-Markov Process based Model

First, the (m+1)-state embedded Markov chain [2,3,47] is developed for the extended Gilbert model as shown in Fig. 6.1. The element P_{ij}^{e} of state transition probability matrix $[\mathbf{P}]^{e}$ of the embedded Markov chain is derived from [47] as follows.

$$P_{ij}^{e} = 0 \quad for\ i = j \tag{6.2.1}$$

$$= \frac{P_{ij}}{(1 - P_{ii})} \quad for\ i \neq j \tag{6.2.2}$$

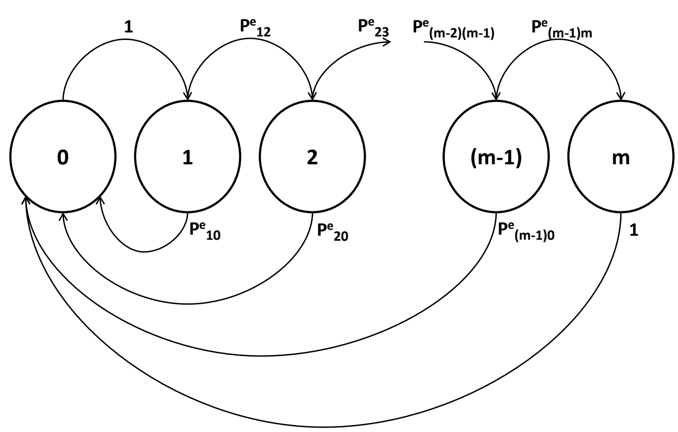

Figure 6.1: The embedded Markov chain for the extended Gilbert model with P_{ii} equal to 0 [2,3].

Thus,

$$[\mathbf{P}]^e = \begin{pmatrix} 0 & 1 & 0 & \cdots & 0 \\ (1-a_1) & 0 & a_1 & \cdots & 0 \\ (1-a_2) & 0 & 0 & \cdots & 0 \\ . & . & . & . & . \\ (1-a_{m-1}) & 0 & 0 & \cdots & a_{m-1} \\ 1 & 0 & 0 & \cdots & 0 \end{pmatrix} \tag{6.2.3}$$

The stationary probability Π_i^e of state i of the embedded Markov chain given by [2, 3, 47]

$$\Pi_i^e = \sum_{j \neq i} \Pi_j^e P_{ji}^e \tag{6.2.4}$$

can be expanded as follows for $i \in (2, m)$ [2, 3]

$$\Pi_0^e = \Pi_1^e P_{10}^e + \Pi_2^e P_{20}^e + \Pi_3^e P_{30}^e + \cdots + \Pi_m^e P_{m0}^e \tag{6.2.5}$$

$$\Pi_1^e = \Pi_0^e P_{01}^e + \Pi_2^e P_{21}^e + \Pi_3^e P_{31}^e + \cdots + \Pi_m^e P_{m1}^e \tag{6.2.6}$$

$$\begin{aligned} \Pi_i^e &= \Pi_0^e P_{0i}^e + \Pi_1^e P_{1i}^e + \cdots + \Pi_{i-1}^e P_{(i-1)i}^e + \Pi_{i+1}^e P_{(i+1)i}^e \\ &+ \cdots + \Pi_m^e P_{mi}^e \end{aligned} \tag{6.2.7}$$

Also,

$$\Pi_0^e + \Pi_1^e + \Pi_2^e + \Pi_3^e + \cdots + \Pi_m^e = 1 \tag{6.2.8}$$

From (6.2.3) through (6.2.8), for $i \in (2, m)$ [2, 3]

$$\Pi_0^e = \frac{1}{(2 + a_1 + a_1a_2 + a_1a_2a_3 + \cdots + a_1 \cdots a_{(m-1)})} \tag{6.2.9}$$

$$\Pi_1^e = \frac{1}{(2 + a_1 + a_1a_2 + a_1a_2a_3 + \cdots + a_1 \cdots a_{(m-1)})} \tag{6.2.10}$$

$$\Pi_i^e = \frac{a_1 \cdots a_{(i-1)}}{(2 + a_1 + a_1a_2 + a_1a_2a_3 + \cdots + a_1 \cdots a_{(m-1)})} \tag{6.2.11}$$

The state holding time H_i of burst loss state i is defined as the time spent by the queue in the burst loss state i before transitioning to another state [2, 47]. The mean state holding time $E[H_i]$ of state i is given by [2]

$$E[H_i] = \frac{Total\ time\ spent\ in\ state\ i}{Total\ number\ of\ transitions\ from\ state\ (i-1)\ to\ state\ i} \tag{6.2.12}$$

The stationary probability Π_i^s of state i of the $(m+1)$-state semi-Markov process is given by [2, 47]

$$\Pi_i^s = \frac{\Pi_i^e \times E[H_i]}{\sum_{j=0}^{m}\{\Pi_j^e \times E[H_j]\}} \tag{6.2.13}$$

6.2.1 Significance of Mean State Holding Time

The drawback of the extended Gilbert model is that it computes the burst loss probabilities assuming packet arrivals at the queue with a unit inter-arrival time. This model does not include a time-dependent parameter to trace the interval between successive arrivals at the queue. The Semi-Markov process compensates for this deficiency using the parameter *state holding time*. This process models the packet inter-arrival time as state holding time, and considers the packet inter-arrival time for computing burst loss probabilities.

6.3 Experimental Setup and Simulations

This section discusses the experiments performed to describe burst losses and to illustrate the effect of packet inter-arrival times on the length of burst losses [2, 3]. Furthermore, the difference between the extended Gilbert model and the semi-Markov process is explained through the simulation results [2]. The experimental testbed consisted of a network of four Cisco routers RA, RB, RC, and RD connected as shown in Figure 6.2. RA is a Cisco 2651 router, whereas RB, RC and RD are Cisco

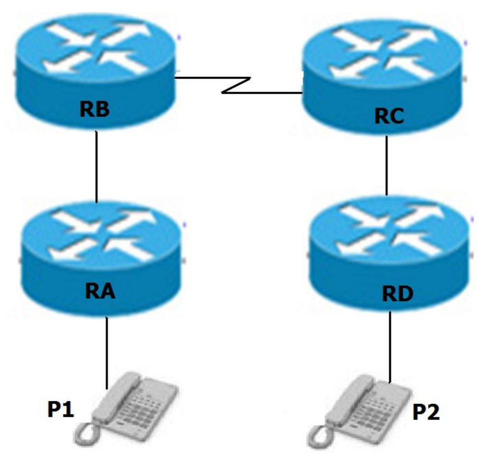

Figure 6.2: The simulation testbed consisting of four Cisco routers and two analog phones. RA is a Cisco 2651 router, and RB, RC, and RD are Cisco 2621 routers [2,3].

2621 routers. Two analog phones P1 and P2 are connected to routers RA and RD, respectively. The two routers RA and RD are enabled with dial-peer configurations to allow the phones to communicate with each other on the IP network. The routers adopt $H.323$ voice signaling mechanisms for logical channel setup. The dial-peer configuration also enables the selection of voice codec for transmissions. In these simulations, the codec G.729 is employed. The dial-peer configurations of router RA and router RD are presented in Table 6.1 [2].

All the routers in the network have the default queue capacity of 75 and 40 for input and output buffers, respectively. FIFO queuing is implemented on all routers. The routers are not configured to provide resource reservation for voice traffic. As the end users initiate the conversation, the codec generates fixed size voice packets at a

Table 6.1: Dial-peer configuration on routers RA and RD [2, 3]

Router-RA	Router-RD
dial-peer voice 222 pots destination-pattern 111 port 1/0/0 exit dial-peer voice 111 voip destination-pattern 222 session target ipv4:192.10.12.3 exit	dial-peer voice 111 pots destination-pattern 222 port 1/0/0 exit dial-peer voice 222 voip destination-pattern 111 session target ipv4:192.10.10.2 exit

constant rate. The router RA is also configured with an application called Pagent to generate data traffic destined to router RD. The Pagent configurations on RA allow the creation of identical data streams which were varied from 5000 to 10000 in steps of 1000 for a fixed packet generation rate. The simulations were carried out for five different packet generation rates. Table 6.2 presents the Pagent configurations on router RA.

Each of these data streams consists of numerous packets with a time gap of one millisecond [2, 3]. This configuration of voice and data traffic was executed for five minutes to complete one scenario. By maintaining the voice call with a constant traffic rate, the data traffic rate is varied by increasing the number of flows configured with a constant rate to cause congestion at the router RB. As the packet arrives at the router's queue, the incoming packet is either accepted into the queue or it is dropped, depending on the status of the queue. The experiments were conducted for two different data transmission rates for six data stream values, and the packet loss traces are captured. These traces are processed to obtain the state transition count V_i for

Table 6.2: Pagent configuration on router RA [2, 3]

Router RA
tgn Add IP
tgn name "B1-50-449-300"
tgn on
tgn interval 1
tgn delayed-start 1 milliseconds
tgn burst on
tgn burst duration on 1000 to 1000
tgn burst duration off 1000 to 1000
!
tgn length 88
!
tgn L2-dest-addr 0000.2222.2223
tgn L2-src-addr 0000.3333.3333
!
tgn L3-version 4
tgn L3-src-addr 192.10.10.2
tgn L3-dest-addr 192.10.12.3

any state i and the state holding time H_i for state i. The state transition probability matrix is derived from (5.3.1), (5.3.2), (5.3.3), and (5.3.4). The stationary probability vector Π is computed for the extended Gilbert model. By computing the mean state, holding times for various states of the extended Gilbert model are then obtained. The stationary probability vector for the semi-Markov process is then computed from (6.1.13) using the mean state holding time $E[H_i]$ and the stationary probability vector Π of the extended Gilbert model. While the length of burst losses in the simulations varied from 0 through 10, the burst losses with a maximum length of 5 were considered in this analysis. Therefore, the state diagram for the semi-Markov process for these scenarios consists of six states, 0 through 5 [2, 3].

6.3.1 Initial State Probability Vector

Table 6.3 presents five initial state probability vectors (Π^0) used in the simulations for computing the stationary probability vector (Π) of the extended Gilbert model [3]. For different initial state probability vectors, the extended Gilbert model converges at different time instances ($n < 100$), however, leading to a unique stationary probability vector. Assuming n to be 100, the stationary probabilities for the extended Gilbert model were computed. Assuming the router's queue to be initially empty, the initial state probability vector of $[1.0, 0, 0, 0, 0, 0]$ was used for computing stationary probabilities [3].

Table 6.3: Initial State Probability Vectors (ISPV) [3]

ID	Initial State Probability Vector
1	[1.0, 0, 0, 0, 0, 0]
2	[0.5, 0.5, 0, 0, 0, 0]
3	[0.3, 0.7, 0, 0, 0, 0]
4	[0.7, 0.3, 0, 0, 0, 0]
5	[0, 1.0, 0, 0, 0, 0]

Table 6.4: State Transition Probability Matrix for Scenario One [2, 3]

	0	1	2	3	4	5
0	0.6487	0.3513	0	0	0	0
1	1	0	0	0	0	0
2	0	0	0	0	0	0
3	0	0	0	0	0	0
4	0	0	0	0	0	0
5	0	0	0	0	0	0

Tables 6.4 through 6.13 present the simulation results. Tables 6.4, 6.6, 6.8, 6.10, and 6.12 show a state transition probability matrix corresponding to the extended

Table 6.5: Mean state holding time (in ms) and stationary probabilities (SP) for extended Gilbert model (eGm) and semi-Markov process (sMp) for scenario one [2,3]

State i of the system	0	1	2	3	4	5
SP for eGm	0.7400	0.2600	0	0	0	0
Mean state holding time (in ms)	25	14.334	0	0	0	0
SP for sMp	0.6356	0.3644	0	0	0	0

Gilbert model for scenarios one, two, three, four, and five. Any entry (i,j) of state transition matrix represents the queue transition probability from state i to j. Tables 6.5, 6.7, 6.9, 6.11, and 6.13 show the stationary probabilities corresponding to the extended Gilbert model and the semi-Markov process for scenarios one through five, respectively [3].

Table 6.6: State Transition Probability Matrix for Scenario Two [2,3]

	0	1	2	3	4	5
0	0.2895	0.7105	0	0	0	0
1	0.1482	0	0.8518	0	0	0
2	0.6522	0	0	0.3478	0	0
3	0.6250	0	0	0	0.375	0
4	0.6664	0	0	0	0	0.3336
5	1	0	0	0	0	0

Table 6.7: Mean state holding time (in ms) and stationary probabilities (SP) for extended Gilbert model (eGm) and semi-Markov process (sMp) for scenario two [2,3]

State of the system	0	1	2	3	4	5
SP for eGm	0.38	0.27	0.23	0.08	0.03	0.01
Mean state holding time (in ms)	25.062	19.825	17.810	11.9623	10.989	7.863
SP for sMp	0.3849	0.3045	0.2330	0.0544	0.0187	0.0045

Table 6.8: State Transition Probability Matrix for Scenario Three [2,3]

	0	1	2	3	4	5
0	0.077	0.9230	0	0	0	0
1	0.125	0	0.875	0	0	0
2	0.8096	0	0	0.1904	0	0
3	1.0	0	0	0	0	0
4	0	0	0	0	0	0
5	0	0	0	0	0	0

Table 6.9: Mean state holding time (in ms) and stationary probabilities (SP) for extended Gilbert model (eGm) and semi-Markov process (sMp) for scenario three [2,3]

State of the system	0	1	2	3	4	5
SP for eGm	0.3377	0.3112	0.2823	0.0688	0	0
Mean state holding time (in ms)	20.64	20.06	20.00	13.5815	0	0
SP for sMp	0.3414	0.3318	0.2894	0.0374	0	0

Table 6.10: State Transition Probability Matrix for Scenario Four [2,3]

	0	1	2	3	4	5
0	0.2608	0.7392	0	0	0	0
1	0.1177	0	0.8823	0	0	0
2	0.6	0	0	0.4	0	0
3	0.5	0	0	0	0.5	0
4	0.6667	0	0	0	0	0.3333
5	1	0	0	0	0	0

Table 6.11: Mean state holding time (in ms) and stationary probabilities (SP) for extended Gilbert model (eGm) and semi-Markov process (sMp) for scenario four [2,3]

State of the system	0	1	2	3	4	5
SP for eGm	0.3445	0.2548	0.2248	0.0899	0.0630	0.0230
Mean state holding time (in ms)	23.935	18.5569	17.99	13.5	11.3170	9.0025
SP for sMp	0.3646	0.2826	0.2418	0.0726	0.0304	0.0080

Table 6.12: State Transition Probability Matrix for Scenario Five [2,3]

	0	1	2	3	4	5
0	0.1112	0.8888	0	0	0	0
1	0.1563	0	0.8437	0	0	0
2	0.9260	0	0	0.0740	0	0
3	0	0	0	0	1	0
4	0.5	0	0	0	0	0.5
5	1	0	0	0	0	0

Table 6.13: Mean state holding time (in ms) and stationary probabilities (SP) for extended Gilbert model (eGm) and semi-Markov process (sMp) for scenario five [2,3]

State of the system	0	1	2	3	4	5
SP for eGm	0.3627	0.3065	0.2576	0.0273	0.0273	0.0186
Mean state holding time (in ms)	24.228	20.120	19.626	10.443	10.443	9.501
SP for sMp	0.3876	0.3219	0.2649	0.0104	0.0104	0.0048

6.3.2 Analysis of Simulation Results

This subsection describes the cause of burst losses and the effect of packet inter-arrival time on the length of burst losses. Furthermore, the difference between extended Gilbert model and the proposed model is illustrated through the simulation results [2, 3]. Tables 6.5, 6.7, 6.9, 6.11, and 6.13 present the stationary probabilities of extended Gilbert model, the mean state holding times and the stationary probabilities of semi-Markov process [3]. Figures 6.3 and 6.4 present the stationary probabilities of extended Gilbert model and semi-Markov process for scenarios two through five [3].

Consider the Table 6.7. When the packets arrived at the congested queue with an average inter-arrival time of 25.062ms, these packets were accommodated in the queue. When the average packet inter-arrival time reduced to 19.825ms, the queue experienced packet drops.

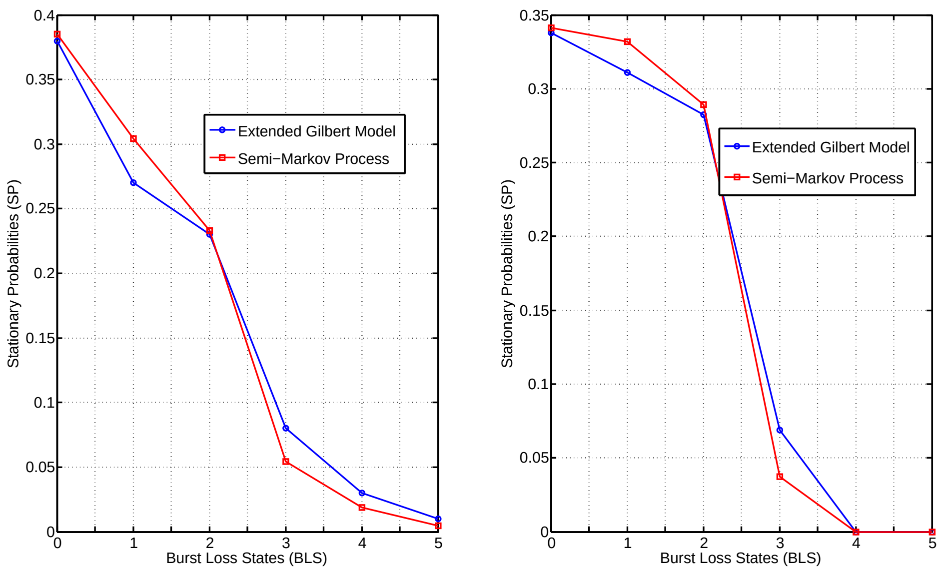

Figure 6.3: (a) Stationary Probabilities for eGm and sMp for Scenario Two [3]. (b) Stationary Probabilities for eGm and sMp for Scenario Three [3].

As the average packet inter-arrival times further reduced, the router queue experienced burst losses of varying lengths. For an average packet inter-arrival times of 7.863ms, the length of burst losses reached a value of five. Similar patterns were also observed in other scenarios as shown in the tables. Hence, it can be observed that a smaller packet inter-arrival time at the congested queue resulted in burst losses. The stationary probabilities of the semi-Markov process represent the probabilities of burst losses of specific lengths for the corresponding average packet inter-arrival times at the queue. Therefore, the stationary probabilities decreased from state zero through state five.

The simulation results show that the semi-Markov process better explains the burst losses and the their dependencies on the packet inter-arrival time [2, 3]. For

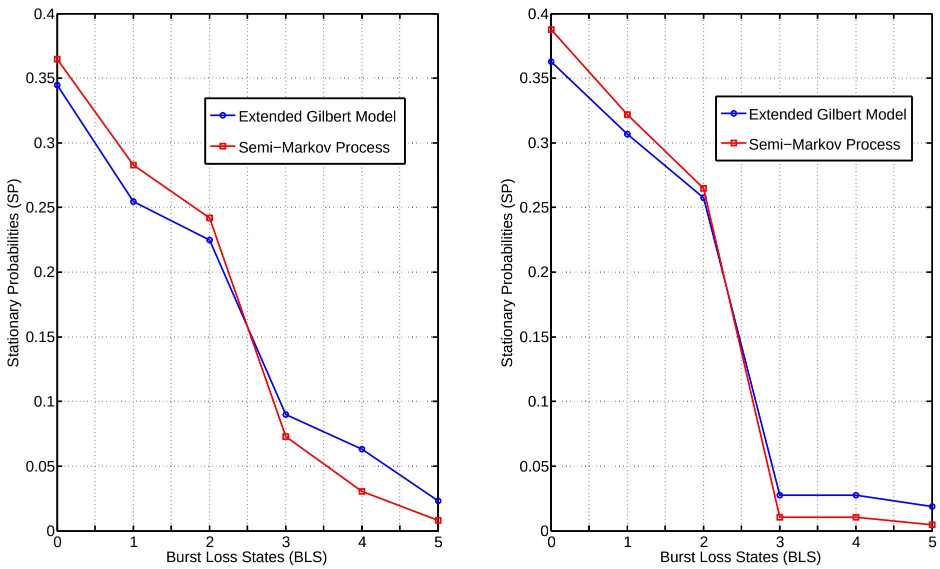

Figure 6.4: (a) Stationary Probabilities for eGm and sMp for Scenario Four [3]. (b) Stationary Probabilities for eGm and sMp for Scenario Five [3].

the specific pattern of average packet inter-arrival times, the semi-Markov process computes the burst loss probability. However the extended Gilbert model lacks this ability. It computes the burst loss probabilities without considering the packet inter-arrival times [2, 3].

6.4 Conclusions

In the existing literature, the extended Gilbert model is used to predict packet losses based on the router queue status. As this model assumes the packet arrivals to occur with a unit time-gap, it lacks the ability to model the queue's response to other packet arrival patterns. In this chapter, the state holding time is introduced into the extended Gilbert model to present an extension to his empirical model for capturing the dependency of burst packet losses on packet inter-arrival times. By incorporating the mean state holding time into this model, the capability of the extended Gilbert model is significantly increased in computing the burst loss probabilities for the variations in the packet inter-arrival patterns. Simulation results were used to illustrate the burst losses and the effect of packet inter-arrival times on the length of burst losses. Also, the simulation results reveal that the length of these losses increased with a decrease in mean state holding time.

Chapter 7

Conclusions and Future Work

7.1 Conclusions

This dissertation analyzed the important aspects of computer networks, such as the packet service-time and burst packet losses in IP networks. The first part of this research proposed an analytical model to describe packet delays in stationary and mobile ad hoc networks, and highlighted the effect of MAC delays on route discovery time and node packet service-time. The second part presented a semi-Markov process based model to analyze the IEEE wireless local area networks (WLANs) and the MAC protocols such as the IEEE 802.11 Distributed Coordination Function (DCF) used in these networks. The third part of the dissertation presented an empirical model to describe the burst losses in Voice over Internet Protocol (VoIP) caused by queue overflows on Internet routers. These models facilitate (a) describing the inter-dependencies of the delays in stationary and mobile ad hoc networks, (b) computing the network parameters of interest for wireless LANs with significant reduction in complexity (from an order of $O(2^m)$ to $O(m)$), and (c) demonstrating the effect of packet inter-arrival times on the length of burst losses. This research lays the foundation for the development of new protocols and algorithms to enhance the network performance.

7.2 Future Work

The research presented in this dissertation can be further extended to (a) model the effect of the IEEE 802.11e Enhanced Distributed Channel Access (EDCA) mechanism on the route discovery time and packet service-time in stationary and mobile ad hoc networks, (b) model the performance of the WLANs employing the IEEE 802.11e Enhanced Distributed Channel Access (EDCA) using the semi-Markov process based model proposed in chapter four of this dissertation work, and (c) model the burst losses in real-time applications on IP networks using the CTMC as presented in the following subsection.

7.2.1 Model and Analysis of Burst Losses in Real-Time Applications Using Continuous-Time Markov Chain

Burst losses were described using several empirical models based on Markov Chains and Semi-Markov process as discussed in chapters five and six. These models can not explain effect of the packet arrival rates, the packet service rates, and the queue capacity on burst losses. This kind of analysis is very important to identify and manage the network resources to regulate the burst losses below a specific length on the bursty network such as the Internet. In this subsection, the burst losses in voice networks are modeled using two-dimensional CTMC [4]. Figure 7.1 shows the CTMC used to model burst losses at a router with queue capacity l. The packet arrivals at the queue follow Poisson distribution, and the packet inter-arrival times and packet service-times follow exponential distribution. Let λ be the mean packet arrival-rate and μ be the mean packet service-rate at the router. The proposed CTMC consists of $[(l+1)m+l]$ states where $1 \leq l < \infty$. Any state (i,j) of the CTMC indicates that the queue observed i consecutive packet losses and it currently holds j packets, $0 \leq i \leq m$ and $0 \leq j \leq l$; m is the maximum consecutive burst losses and $1 \leq m < \infty$ [4]. Initially, when the queue is full with l packets in it, the burst loss state is represented as $(0,l)$. When a new packet arrives at the queue, the burst loss state changes from $(0,l)$ to $(1,l)$ because of a packet loss. Now, if the queue serves a packet, then the burst loss state becomes $(1,l-1)$. In this state, if a new packet arrives at the queue, then the queue accommodates the packet and the burst loss state becomes $(0,l)$ [4].

The state transition from $(0,j-1)$ to $(0,j)$ indicates that a new packet is accommodated into the router, whereas the transition from $(0,l)$ to $(1,l)$ represents a packet loss after a new packet arrival. The possible transitions from state (i,j), $1 \leq i \leq (m-1)$ and $0 \leq j \leq l$, are to the states $(i+1,j)$ and $(i,j-1)$, representing an arrival or servicing of a packet, respectively. The packet inter-arrival time at the router is modeled as state holding time of various states in the CTMC. Therefore, the state transition rates for CTMC in Figure 2 are [4]

$$q_{(i,l),(i+1,l)} = \lambda, \quad for\ 0 \leq i \leq (m-1) \tag{7.2.1}$$

$$q_{(m,l),(0,l)} = \lambda \tag{7.2.2}$$

$$q_{(i,j),(i,j-1)} = \mu, \quad for\ 1 \leq i \leq m,\ 0 \leq j \leq l \tag{7.2.3}$$

$$q_{(i,j),(0,j+1)} = \lambda, \quad for\ 0 \leq i \leq m,\ 1 \leq j \leq l \tag{7.2.4}$$

The steady-state probability vector Π for the proposed CTMC is obtained by solving

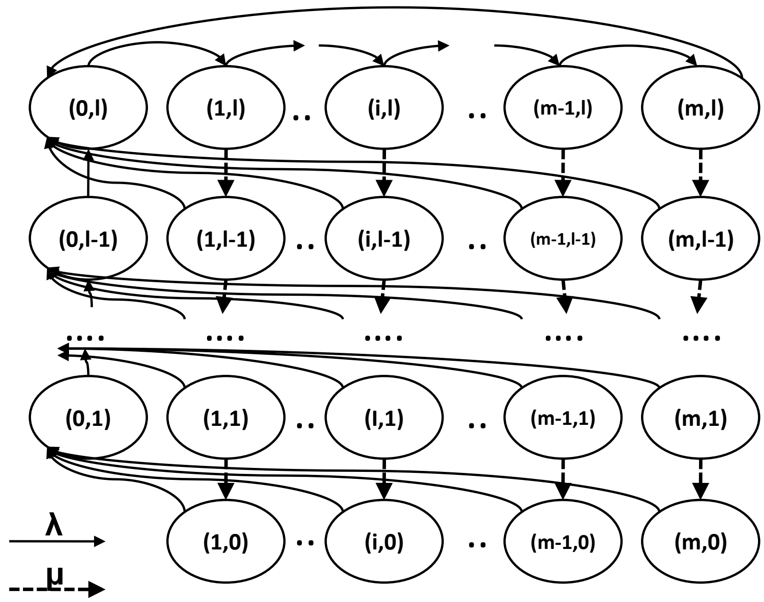

Figure 7.1: Continuous-Time Markov Chain describing burst losses at a queue with capacity l in voice networks; l is finite and $0 \leq l < \infty$. The state transition from burst loss state (i, l) to $(i+1, l)$, $0 \leq i \leq (m-1)$, represents a new packet loss. m represents the maximum length of burst loss at the queue; m is finite and $0 \leq m < \infty$. The state transition from burst loss state (m, l) to $(0, l)$ indicates that the burst loss length is reset to 0 after a burst loss of length $(m+1)$. The state transition from burst loss state (i, j) to $(i, j-1)$, $1 \leq i \leq m$ and $0 \leq j \leq l$, indicates that a queued packet was served. The state transition from burst loss state $(0, j-1)$ to $(0, j)$ indicates that the number of packets in the queue is j [4].

the set of equations given by [4]

$$\Pi Q = 0 \tag{7.2.5}$$

$$\sum_{j=1}^{l} \Pi_{(0,j)} + \sum_{i=1}^{m} \sum_{j=0}^{l} \Pi_{(i,j)} = 1 \tag{7.2.6}$$

Let

$$x = \frac{\lambda}{\lambda + \mu}; y = \frac{\mu}{\lambda + \mu} \tag{7.2.7}$$

Using the flow-balance equations, the stationary probabilities are computed for $1 \le i \le m$ and $1 \le j \le l$ as follows [4].

$$\Pi_{(i,l)} = \Pi_{(0,l)} \times x^i; \Pi_{(i,l-j)} = \Pi_{(0,l)} \times x^i y^j \tag{7.2.8}$$

$$\Pi_{(i,0)} = \Pi_{(i,l-l)} = \Pi_{(0,l)} \times x^{(i-1)} y^l \tag{7.2.9}$$

Similarly [4]

$$\Pi_{(0,l)} = \sum_{i=0}^{m} \Pi_{(i,l-1)} + \Pi_{(m,l)} \tag{7.2.10}$$

$$\Pi_{(0,1)} = \Pi_{(0,l-(l-1))} = \sum_{i=1}^{m} \Pi_{(i,0)} = \Pi_{(0,l)} \left\{ \frac{1-x^m}{1-x} \right\} y^l \tag{7.2.11}$$

$$\Pi_{(0,l-j)} = \sum_{i=0}^{m} \Pi_{(i,j-1)},\ 1 \le j \le (l-2) \tag{7.2.12}$$

The sum of stationary burst loss probabilities associated with a desired burst loss length i, denoted as Π_i, is computed as follows [4].

$$\Pi_0 = \sum_{j=0}^{(l-1)} \Pi_{(0,l-j)}; \quad \Pi_1 = \sum_{j=0}^{l} \Pi_{(1,j)} = \Pi_{(0,l)} \tag{7.2.13}$$

$$\Pi_2 = \sum_{j=0}^{l} \Pi_{(2,j)} = \Pi_{(0,l)} \times x \tag{7.2.14}$$

$$\Pi_i = \sum_{j=0}^{l} \Pi_{(i,j)} = \Pi_{(0,l)} \times x^{(i-1)},\ 1 \le i \le m \tag{7.2.15}$$

The sum of all stationary burst loss probabilities is equal to 1. Solving

$$\sum_{i=0}^{m} \Pi_i = 1 \tag{7.2.16}$$

we obtain the $\Pi_{(0,l)}$, which can be substituted in (7.2.8) through (7.2.12) to obtain the stationary burst loss probabilities $\Pi_{(i,j)}$ [4].

Substituting $\Pi_{(0,l)}$ in (7.2.13)-(7.2.15), the stationary probability Π_i of occurrence of burst loss of length i is obtained [4].

We define the state holding time H_i for state i as the time interval for which the length of burst losses i (first component of state (i,j)) remains constant $0 \leq i \leq m$, irrespective of the number of packets j available in the queue. Let $H_{(i,j)}$ be the state holding time of state (i,j) which is the time interval for which the length of burst loss remains i with j packets stored in the queue. $H_{(i,j)}$ is exponentially distributed with parameter $(\lambda+\mu)$ for all $i > 0$ and $j > 0$. From state (i,j), the next transition occurs to state $(i, j-1)$ for $i > 0$ and $j > 0$ with probability $\frac{\mu}{\lambda+\mu}$ and to state $(0, j+1)$ with probability $\frac{\lambda}{\lambda+\mu}$. Also, $E[H_{(i,j)}] = 1/(\lambda+\mu)$ for $i > 0$ and $j > 0$ and $E[H_{(i,j)}] = 1/\lambda$ for $i = 0$ or $j = 0$. Hence, the expected state holding time $E[H_i]$ for the burst loss state i $(i > 0)$ is given by [4]

$$E[H_i] = E[H_{(i,l)}] + \frac{\mu}{(\lambda+\mu)} \left\{ E[H_{(i,l-1)}] + \frac{\mu}{(\lambda+\mu)} E[H_{(i,l-2)}] + \ldots + \left\{ \frac{\mu}{(\lambda+\mu)} \right\}^{(l-1)} E[H_{(i,0)}] \right\}$$

The expected value $E[H_0]$ of state holding time for state 0 can be similarly computed [4].

7.2.2 Applicability of the Proposed Model

For a fixed λ, μ, l, and m, the expected length E_L of burst losses can be computed as [4]

$$\begin{aligned} E_L &= \sum_{i=0}^{m} i\Pi_i = \Pi_1 + 2\Pi_2 + \ldots + m\Pi_m \qquad (7.2.17) \\ &= \Pi_{(0,l)} + 2x\Pi_{(0,l)} + 3x^2\Pi_{(0,l)} + \ldots + mx^{(m-1)}\Pi_{(0,l)} \end{aligned}$$

$$
\begin{aligned}
E_L &= \Pi_{(0,l)}\{1 + 2x + 3x^2 + \ldots + mx^{(m-1)}\} \\
&= \Pi_{(0,l)}\left\{\frac{mx^m}{(x-1)} - \frac{1}{(x-1)} - \frac{(x^m - x)}{(x-1)^2}\right\} \\
&= \Pi_{(0,l)}\left\{\frac{mx^{(m+1)} - (m+1)x^m + 1}{(x-1)^2}\right\} \qquad (7.2.18)
\end{aligned}
$$

Simplifying, we get the expected length E_L of burst loss as [4]

$$
\Pi_{(0,l)}\left\{\frac{(\lambda+\mu)^{(m+1)} - \lambda^{(m+1)} - (m+1)\lambda^m\mu}{\mu^2(\lambda+\mu)^{(m-1)}}\right\} \qquad (7.2.19)
$$

Therefore, for a fixed capacity l, maximum length of burst losses m, and mean packet service-rate μ at the router's queue, E_L is a function of packet arrival-rate λ. Thus, the mean packet arrival-rate λ that can regulate the length of burst losses E_L below a desired length can be computed.

This subsection presented a CTMC based model for describing the effect of packet arrival-rate, packet service-rate, and queue capacity on the burst losses in real-time applications such as VoIP. It also computes the parameters of interest related to burst losses such as the stationary burst loss probabilities, expected length of burst losses. Furthermore, the proposed model computes acceptable range of packet arrival-rates that can restrict the burst losses below desired lengths. Hence, the proposed model contributes significantly towards provisioning the required resources at the Internet router to accommodate bursty voice traffic. This model will be validated through the real-time testbed scenarios.

REFERENCES

REFERENCES

[1] M. K. Kadiyala, D. Shikha, R. Pendse, and N. Jaggi, “ Semi-Markov process based model for performance analysis of wireless LANs” *Proceedings of Seventh IEEE PerCom Workshop on Pervasive Wireless Networking (PWN 2011)*, Mar 2011.

[2] M. K. Kadiyala, R. Pendse, and K. Namuduri, “On the dependence of the burst losses on the packet inter-arrival times in VoIP”, *Proc. of IEEE Globecom 2010 Workshop on Multimedia Communications and Services, Dec 2010.*

[3] M. K. Kadiyala, R. Pendse, and K. Namuduri, “On the impact of the packet inter arrival-times on burst loss patterns in VoIP”, *Submitted to Springer: Journal of Inter Services and Applications, Jan 2011.*

[4] M. K. Kadiyala, N. Jaggi, R. Pendse, and K. Namuduri, “Model and analysis of burst losses in real-time applications using CTMC”, *Ready for submission to IEEE Communications Letters, May-June 2011*

[5] M. K. Kadiyala, and R. Pendse, “ Cross-layer analysis of route discovery processes and its impact on packet end-to-end delay in wireless ad hoc networks”, *Proc. of IEEE Vehicular Technology Conference, Fall 2006, September 2006*

[6] M. K. Kadiyala, S. Paradi, and R. Pendse, “The impact of medium access delays on packet service-time in saturated ad hoc networks”, *Proc of IEEE International Workshop on Wireless Local Networks, Oct 2010*

[7] M. K. Kadiyala, U. Siddiqui, and R. Pendse, “The quantitative analysis of queuing delays in saturated ad hoc networks”, *Ready for submission to the Springer Journal on distributed Computing, May-June 2011*

[8] M. K. Kadiyala, N. Chandna, and R. Pendse, “On the quantitative analysis of frame inter-arrival times in stationary ad hoc networks”, *Ready for submission to the IEEE Communications Letters, May-June 2011.*

[9] M. K. Kadiyala, H. Shah, and R. Pendse, “Cross-layer analysis of the route discovery process in saturated ad hoc networks”, *Ready for the submission to the Springer Journal on Distributed Computing, May 2011.*

[10] Giuseppe Bianchi, “Performance analysis of the IEEE 802.11 distributed coordination function” *IEEE Journal on Selected Areas in Communications*, vol. 18, no. 3, pp. 535-547, March 2000.

REFERENCES (continued)

[11] F. Alizadeh-Shabdiz and S. Subramaniam, “A finite load analytical model for the IEEE 802.11 distributed coordination function MAC", *Proceedings WiOpt'03: Modeling and Optimization in Mobile, Ad Hoc and Wireless Networks*, France, March 2003

[12] B.-J. Kwak, N.-O. Song, and L. E. Miller, “Analysis of the stability and performance of exponential backoff", *Proceedings. IEEE Wireless Communication and Networking Conference (WCNC'03)*, New Orleans, LA, March 2003

[13] *H. Chen and Y. Li, “*Performance model of IEEE 802.11 DCF with variable packet length*", IEEE Communications Letters,* vol. 8, no. 3, pp. 186-188, March 2004.

[14] *C. H. Foh and J. W. Tantra, “*Comments on IEEE 802.11 saturation throughput analysis with freezing of back off counters", *IEEE Communication Letters,* vol. 9, no. 2, pp. 130-132, February 2005.

[15] X. J. Dong and P. Varaiya, “Saturation throughput analysis of IEEE 802.11 wireless LANs for a lossy channel", *IEEE Communication Letters*, vol. 9, no. 2, pp. 100-102, February 2005.

[16] O. Tickoo and B. Sikdar, “Queuing analysis and delay mitigation in IEEE 802.11 random access MAC based wireless networks", *Proc. IEEE INFOCOM'04*, Hong Kong, China, March 2004.

[17] O. Tickoo and B. Sikdar, “A queuing model for finite load IEEE 802.11 random access MAC", *Proc. IEEE International Conference on Communications (ICC'04)*, Paris, France, June 2004.

[18] S. G. Sitharaman, “*Modeling queues using Poisson approximation in IEEE 802.11 ad hoc networks*"

[19] A. Abdrabou and W. Zhuang, “Service time approximation in IEEE 802.11 single-hop ad hoc networks", *IEEE INFOCOM, 2007.*

[20] M. A. Rabou Kalil, H. Al-Mahdi, and A. Mitschele-Thiel, “*Modeling of an efficient queue management scheme for multihop ad hoc networks*",

[21] B. Li and R. Battiti, “Performance analysis of an enhanced IEEE 802.11 distributed coordination function supporting service differentiation", *Proc. International Workshop on Quality of Future Internet Services (QoFIS'03)*, pp. 152-161, October 2003.

[22] H. Zhu and I. Chlamtac, “An analytical model for IEEE 802.11e EDCF differential services", *Proc. 12th International Conference on Computer Communications and Networks (ICCCN'03)*, Dallas, TX, October 2003.

[23] M. Heusse, F. Rousseau, G. Berger-Sabbatel, and A. Duda, “Performance anomaly of 802.11b", *Proc. IEEE INFOCOM'03*, San Francisco, March-April 2003.

[24] G. R. Cantieni, Q. Ni, C. Barakat, and T. Turletti, “Performance analysis of finite load sources in 802.11b multirate environments”, *Special Issue on Performance Issues of Wireless LANs, PANs, and Ad Hoc Networks*, Elsevier Computer Communications Journal, vol. 28, 2005.

[25] A. Grilo and M. Nunes, “Performance evaluation of IEEE 802.11e”, *Proc.13th IEEE International Symposium on Personal, Indoor, and Mobile Radio Communications (PIMRC'02)*, vol. 1, San Jose, California, September 2002, pp. 511-517.

[26] P. B. Velloso, M. G. Rubinstein, and O. C. M. B. Duarte, “*Evaluating voice traffic requirements on IEEE 802.11 ad hoc networks*”.

[27] I. Inan, F. Keceli, and E. Ayanoglu, “Analysis of the 802.11e enhanced distributed channel access function”, *IEEE Transactions on Communications*, vol. 57, pp. 1753-1764, June 2009.

[28] D. Estrin, D. Culler, K. Pister, and G. Sukhatme, “Connecting the physical world with pervasive networks”, *IEEE Pervasive Computing*, 2002.

[29] S. Tompros, N. Mouratidis, M. Caragiozidis, H. Hrasnica, and A. Gavras, “A pervasive network architecture featuring intelligent energy management of house-holds”, *Proceedings of the 1st international conference on Pervasive Technologies Related to Assistive Environments*, 2008.

[30] N. G. Neumann, “*Two algorithms for leader election and network size estimation in mobile ad hoc networks*”, Master's thesis, Texas A and M University, Dec 2004.

[31] R. Ali, S. Lor, and M. Rio, “Two algorithms for network size estimation for master/slave ad hoc networks”, *IEEE 3rd International Symposium on Advanced Networks and Telecommunication Systems (ANTS),* pp. 1-3, Dec 2009.

[32] R. Nelson, “*Probability, Stochastic Processes and Queuing Theory: Mathematics of Computer Performance and Analysis*”, ser. Springer-Verlag, New York, 1995.

REFERENCES (continued)

[33] J.-C. Bolot, "Characterizing end-to-end packet delay and loss in the Internet", *Journal of High-Speed Networks*, vol. 2, no. 3, pp. 305-323, December 1993.

[34] J.-C. Bolot, H. Crepin, and A. V. Garcia, "Analysis of audio packet loss in the Internet", *Proceedings 5th International Workshop on Network and Operating System Support for Digital Audio and Video*, April 1995, pp. 163-174.

[35] M. Borella, "Measurement and interpretation of Internet packet loss", *Journal on Communication and Networks*, vol. 2, no. 2, pp. 93-102, June 2000.

[36] I. Kaj and I. Marsh, "Modeling the arrival process for packet audio", *Proceedings 2nd Int. Workshop on Quality of Service in Multiservice IP Networks*. Springer-Verlag, 2003, pp. 35-49.

[37] P. Pragtong, K. M. Ahmed, and T. J. Erke, "Analysis and modeling of voice over IP traffic in the real network", *IEICE Transactions on Information and Systems*, vol. E89-D, no. 12, pp. 2886-2896, December 2006.

[38] A. Biernacki, "Stochastic models for VoIP traffic and their applications", *Proceedings of 25th IASTED International multi-Conference*, pp. 145-150, February 2007.

[39] V. P. Koutras and A. N. Platis, "VoIP availability and service reliability through software rejuvenation policies", *Second International Conference on Dependability of computer Systems*, 2007

[40] Y. Lu, Y. H. Zhong, and B. Bhargav, "Packet loss in mobile ad hoc networks", *CSD TR* No.03-009, April 2003.

[41] M. Yajnik, S. Moon, J. Kurose, and D. Towsley, "Measurement and modeling of the temporal dependency in packet loss", *Proceedings IEEE INFOCOM*, March 1999, pp. 345-352.

[42] H. Sanneck and G. Carle, "A framework model for packet loss metrics based on loss runlengths", *Proceedings of the SPIE/ACM SIGMM Multimedia Computing and Networking Conference 2000*, San Jose, CA, USA, January 2000.

[43] W. Jiang and H. Schulzrinne, "*QoS measurement of internet real-time multimedia services*", Columbia University, New York, Tech. Rep. CUCS-015-99, December 1999.

REFERENCES (continued)

[44] W. Jiang and H. Schulzrinne, "Modeling of packet loss and delay and their effect on real-time multimedia service quality", *Proceedings 10th Int. Workshop Network and Operations System Support for Digital Audio and Video*, Chapel Hill, NC, USA, June 2000.

[45] H. Sanneck, N. T. L. Le, A. Wolisz, and G. Carle, "Intra-flow loss recovery and control for VoIP", *Proceedings ACM International Conference on Multimedia. Ottawa*, Canada: ACM Press, 2001, pp. 441-454.

[46] V. S. Frost, "Quantifying the temporal characteristics of network congestion events for multimedia services", *IEEE Trans. on Multimedia*, vol. 5, no. 3, pp. 458-465, September 2003.

[47] R. Nelson, "*Probability, Stochastic processes and Queuing Theory: Mathematics of Computer Performance and Analysis*" Springer-Verlag Series, 1995.